IN VIVO DETECTION OF GPCR DIMERIZATIONS IN *SACCHAROMYCES CEREVISIAE* USING FRET AND BiFC

A THESIS SUBMITTED
TO THE GRADUATE SCHOOL OF NATURAL AND APPLIED SCIENCES
OF
MIDDLE EAST TECHNICAL UNIVERSITY

BY

BEREN ÜSTÜNKAYA

IN PARTIAL FULFILLMENT OF THE REQUIREMENTS
FOR
THE DEGREE OF MASTER OF SCIENCE
IN
BIOLOGY

SEPTEMBER 2014

Approval of the Thesis

***IN VIVO* DETECTION OF GPCR DIMERIZATIONS IN *SACCHAROMYCES CEREVISIAE* USING FRET AND BiFC**

submitted by **BEREN ÜSTÜNKAYA** in partial fulfillment of the requirements for the degree of **Master of Science in Biology Department, Middle East Technical University** by,

Prof. Dr. Canan Özgen _____
Dean, Graduate School of **Natural and Applied Sciences**

Prof. Dr. Orhan Adalı _____
Head of the Department, **Biology**

Assoc. Prof. Dr. Çağdaş Devrim Son _____
Supervisor, **Biology Department, METU**

Examining Committee Members

Prof. Dr. Meral Yücel _____
Biology Department, METU

Assoc. Prof. Dr. Çağdaş Devrim Son _____
Biology Department, METU

Assoc. Prof. Dr. Aysegül Gözen _____
Biology Department, METU

Assoc. Prof. Dr. Tülin Yanık _____
Biology Department, METU

Assist. Prof. Dr. Bala Gür Dedeoğlu _____
Biotechnology Institute, Ankara University

Date: 05.09.2014

I hereby declare that all information in this document has been obtained and presented in accordance with academic rules and ethical conduct. I also declare that, as required by these rules and conduct, I have fully cited and referenced all material and results that are not original to this work.

Name, Last Name :

Signature :

ABSTRACT

IN VIVO DETECTION OF GPCR DIMERIZATIONS IN *SACCHAROMYCES CEREVISIAE* USING FRET AND BiFC

Üstünkaya, Beren
M.S., Department of Biology
Supervisor: Assoc. Prof. Dr. Çağdaş Devrim Son
September 2014, 92 pages

G protein-coupled receptors (GPCRs) are a class of membrane proteins that are composed of seven transmembrane domain and mediate physiological response to a diverse array of stimuli. In eukaryotic microorganisms, GPCRs regulate cell growth, development, morphogenesis, motility, and life span. In higher eukaryotic organisms as humans, they mediate the action of hundreds of peptide hormones, sensory stimuli, odorants, neurotransmitters, and chemokine. Due to their wide spectrum of action mechanisms, GPCRs are also targets for ~40-50% of current pharmaceuticals in the market. For a long time, these receptors have been thought to locate and function as monomeric units which activate a related heterotrimeric G protein to transmit the extracellular signal to inside of the cell. However, recent studies in last two decades have suggested that GPCRs form dimers (or higher order oligomers) for proper trafficking and/or functioning. After these early findings, many studies have been conducted to reveal, examine and understand dimerization of single type or different type of the receptors. So far, the dimers/oligomers have been reported to play important roles in regulation of receptor expression, ligand binding and second messenger activation whereas there is still limited information on how and where GPCR dimerization occurs, which type of them interact with each other, and where these dimers are located in the cells. In this thesis, we studied detection of dimer formation between nutrient sensing GPCR in *Saccharomyces cerevisiae*, Gpr1

proteins with its own type, and also with Ste2 protein, which is expressed as mating pheromone receptor by MAT**a** type of haploid yeast cells. *In vivo* imaging after application of Förster Resonance Energy Transfer (FRET) and Bimolecular Fluorescence Complementation (BiFC) methods successfully showed that both dimer groups are located on plasma membrane and in intracellular compartments as endoplasmic reticulum and Golgi of wild type and mutant strains.

Keywords: BiFC, FRET, GPCR dimerization, Gpr1p, *Saccharomyces cerevisiae*, Ste2p

ÖZ

GPKR DİMERLEŞMESİNİN FRET ve BÖLÜNMÜŞ FLORESAN PROTEİN (BiFC) TEKNİKLERİ İLE CANLI *SACCHAROMYCES CEREVISIAE* HÜCRELERİNDE GÖRÜNTÜLENMESİ

Üstünkaya, Beren
Yüksek Lisans, Biyoloji Bölümü
Tez Yöneticisi : Doç. Dr. Çağdaş Devrim Son
Eylül 2014, 92 sayfa

G-proteine kenetli reseptörler (GPKRler) membran reseptörlerinin, yedi transmembran bölgeden oluşan, çok çeşitli uyaranlara karşı fizyolojik yanıt oluşturulmasını sağlayan bir sınıfıdır. Ökaryot mikroorganizmalarda bulunan GPKRler hücre büyümesi, gelişmesi, morfogenezi, hareketi ve yaşam süresini kontrol ederken, insan gibi daha gelişmiş ökaryot canlılarda, yüzlerce peptit hormonu, duyusal uyaran, odorant, nörotransmitter ve kemokinlerin etki mekanizmalarında önemli rol oynar. Geniş etki mekanizmaları sebebiyle, bu reseptör sınıfı, günümüzde piyasada olan ilaçların yaklaşık olarak %40-50' sinin hedefi halindedir. Uzun yıllar boyunca, bu reseptörlerin, hücre dışından gelen sinyali hücre içerisine iletmek için etkileşimde bulunduğu heterotrimer yapıdaki G proteinlerini aktif hale getirdiği, hücrede monomer yapıda bulunduğu ve çalıştığı düşünülmüştür. Ancak, son yirmi yılda yapılan çalışmalar GPKRlerin, hücrede düzgün paketlenmesi ve çalışması için dimer (ya da daha yüksek yapılı oligomerler) oluşturduğu fikrini gündeme getirdi. Bu ilk bulgulardan sonra, aynı tür ya da farklı tür GPKRler arasında oluşan dimerleşmeyi göstermek, çalışmak ve anlamak amacıyla birçok proje yapıldı. Şimdiye kadar yapılan çalışmalar sonucunda dimer-/oligomerlerin reseptör ifadesinde, ligand bağlanmasında, ve ikincil mesajcı aktivasyonunda önemli rol oynadığı rapor edilirken GPKR dimerlerinin nasıl ve nerede oluştuğu, hangi türleri

arasında dimerleşme görüldüğü konularındaki mevcut bilgi kısıtlı kalmıştır. Bu çalışmada, mayada besin sensör mekanizması olarak çalışan GPKR türünün, Gpr1 proteinlerinin, kendi türü, ve Ste2, MAT**a** hücreleri tarafından sentezlenen feromon reseptörleriyle dimerleşmesini canlı *Saccharomyces cerevisiae* hücrelerinde inceledik. Floresan rezonans enerji transfer ve bölünmüş floresan protein tekniklerinin uygulamasından sonra yapılan *in vivo* görüntülemeler gösteriyor ki, her iki dimer grubu doğal ve mutant suşların plazma membranı ve golgi, endoplazmik retikulum gibi hücre içi yapılarda bulunmaktadır.

Anahtar kelimeler: Bölünmüş Floresan Proteins, FRET, GPKR dimerleşmesi, Gpr1, *Saccharomyces cerevisiae*, Ste2

ACKNOWLEDGMENTS

I would like to thank first and foremost my thesis advisor, Dr. Çağdaş D. Son, for his support and guidance throughout this study. I am grateful for freedom he has given in the lab and his launching me on the path to becoming an independent researcher.

I would like to thank members of thesis examining committee; Dr.Meral Yücel, Dr.Tülin Yanık, Dr.Ayşegül Gözen and Dr. Bala Gür Dedeoğlu for their time, invaluable suggestions and comments which make the final version of the thesis better.

I am really grateful to my ex- and current labmates; İlke Süder, Sinem Çelebiöven, Orkun Cevheroğlu, Selin Akkuzu, Şerife Şeyda Pirinçci, Giray Bulut and Burcu Karakaya for sharing their knowledge, motivating and assisting in every situation. They made the times spent in the lab more fun.

This work is supported by TUBITAK (110T414) and Marie Curie Actions, International Reintegration Grant (IRG).

I would like to express my gratitude for my family, Beril, Berrin and Ender Üstünkaya for their life-long support and effort to stand by me even they are hundreds-km away.

I wish to express my deep appreciation to my dearest friends curly Özge Doğan, Mine Özcan, Tuğçe Özmen and Nilay Köse for their endless support, guidance and help in any case. I have learnt many things from them since the day we met.

Last but not the least; I would like to thank my dear, Emrah Sezer, for his understanding, support, assistance and motivation in any circumstances. It would be truly impossible to write this thesis without him.

TABLE OF CONTENTS

LIST OF TABLES

LIST OF FIGURES

LIST OF ABBREVIATIONS

Bar:	Barrier (to α-factor diffusion)
BiFC:	Bimolecular Fluorescence Complementation
BRET:	Bioluminescence resonance energy transfer
cAMP:	Cyclic adenosine monophosphate
DHFR:	Dihydrofolate reductase
DNA:	Deoxyribonucleic Acid
EDTA:	Ethylenediaminetetraacetic acid
EGFP:	Enhanced Green Florescent Protein
ER:	Endoplasmic Reticulum
EtBr:	Ethidium Bromide
FP:	Fluorescent Protein
FRET:	Fluorescence Resonance Energy Transfer
GABA:	Gamma-Aminobutyric acid
GABAB:	Gamma-Aminobutyric acid type B receptor
GAP:	Glyceraldehyde 3-phosphate
GDP:	Guanosine diphosphate
GEF:	Guanine nucleotide exchange factor
GFP:	Green fluorescent protein
GnRH:	Gonadotropin releasing hormone
GPCR:	G-protein coupled receptor
GPI:	Glycosylphosphatidylinositol
GRK:	GPCR kinase
GTP:	Guanosine triphosphate
LB:	Luria Bertani
LiAc:	Lithium acetate
MAPK:	Mitogen-activated protein kinase
MAT:	Methionine adenosyltransferase
MLT:	Medium lacking tryptophan

MLU: Medium lacking uracil

MLTU: Medium lacking tryptophan and uracil

NTS1: Neurotensin receptor

PAK: p21-activated kinase

PAGE: Polyacrylamide gel electrophoresis

PCR: Polymerase chain reaction

PEG: Polyethylene glycol

PKA: Protein kinase A

PM: Plasma Membrane

SDS: Sodium dodecyl sulfate

TBE: Tris/Borate/EDTA

TEV: Tobacco etch virus

V_2: Vasopressin receptor

YEPD: Yeast Extract-Peptone-Dextrose

CHAPTER I

INTRODUCTION

1.1. G-protein coupled receptors

Membrane proteins located at cell surface are key players in communication of a cell's internal compartments with its external environments (Venkatakrishnan *et al*., 2013). G-protein coupled receptors (GPCRs) form one of the largest and the most diverse family of transmembrane receptors (Kobilka, 2013; Xue *et al*., 2008; Venkatakrishnan *et al*., 2013). Although the members of this family differ in their primary sequences and biological functions, they share the same basic structure consisting of seven transmembrane domains (TMs) and similar mechanisms of signal transduction (Xue *et al*., 2008). GPCRs, known as the most versatile membrane sensors in nature, respond to plenty of endogenous and exogenous stimulants including, but not limited to, ions, lipids, biogenic amines, odorants, photons and therapeutic drugs. After agonist binding, these receptors convert the signal into cellular responses via major pathways involving G proteins, GPCR kinases (GRKs), arrestins, and homomeric and/or heteromeric interactions with other GPCRs (Heng *et al*., 2014).

Activated GPCRs are coupled by a membrane bound heterotrimeric G protein which consists of α-, β- and γ-subunits and act as a guanine nucleotide exchange factor to exchange of GDP for GTP on G protein α-subunit (Wettschureck and Offermanns, 2005). This exchange leads to dissociation of GTP bound Gα from the receptor as well as from the βγ-subunits, and both subunit complexes activate distinct downstream effectors (Dorsam and Gutkind, 2007; Wettschureck and Offermanns, 2005). The diversity of GPCR signaling arises from their distinct types of ligands

and different subfamilies of α-subunits of interacting G proteins, which are listed in Figure 1.1. (Dorsam and Gutkind, 2007). GPCR signaling mediates the majority of cellular responses to hormones, neurotransmitters and chemokines, and control fundamental biological and pathological processes in cardiovascular, neural, endocrine and immune systems. Since these membrane proteins play key roles in different systems of the human body, they are major focus of drug research for various clinical pathologies as metabolic disorders, inflammation, neurodegenerative disorders, infectious diseases and cancer (Heng *et al*., 2014; Rosenbaum, Rasmussen and Kobilka, 2009). Today, approximately 40 % of clinically approved drugs on the market are designed to mediate their effects via GPCRs (Eglen and Reisine, 2009).

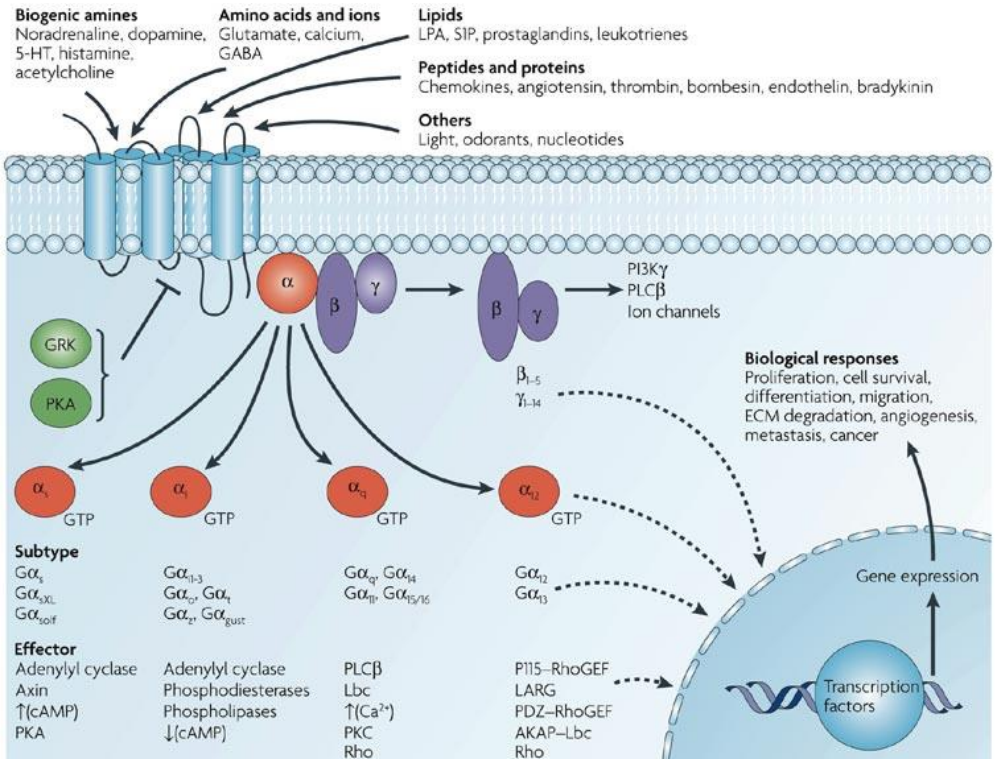

Figure 1.1 The diversity of ligands and regulator molecules in human GPCR signaling systems (Dorsam and Gutkind, 2007)

1.1.1. GPCRs in Saccharomyces cerevisiae

Although more than 1,000 of the ~22,000 genes in humans encode GPCRs, only three of ~5,900 genes in the *Saccharomyces cerevisiae* encode receptors of this class (Fredriksson and Schiöth, 2005; Blumer *et al*., 2007). The protein products of these three genes are Ste2p, Ste3p and Gpr1p (Dohlman and Thorner, 2001). In yeast, GPCR signaling mediates two fundamental biological processes: conjugation and nutrient sensing (Thevelein *et al*., 2005). Ste2 protein is identified as α-factor receptor expressed only by one type of haploid yeast cells, **a-** mating type, and Ste3 protein is a-factor receptor expressed only by cells of **α**-mating type. Unlike these GPCRs of pheromone signaling pathway, Gpr1 protein is expressed by both type of haploid cells and is responsible for nutrient sensing (Blumer *et al*., 2007).

1.1.1.1. Gpr1p, glucose sensing receptor

In nature, glucose is the primary choice of carbon and energy source for most of the cells, as well as yeast cells (Xue *et al*., 1998). The main reason of the preference of glucose (also related rapidly fermented sugars, like fructose and mannose) , and fermentation as metabolic pathway for these sugars by yeast cells is to maintain the fastest growth rate. Although the transportation and catabolism of these sugars regulated by multiple pathways triggered by these sugars, at the end of each pathway, the main goal is to stimulate both fermentation and cell proliferation (Rolland *et al*., 2001, 2002).

In *S.cerevisiae*, two distinct types of membrane proteins functioning as glucose sensors have been discovered: transporter homologues developing into non-transporting glucose sensors, and a glucose-sensing GPCR, Gpr1p (Peeters and Thevelein, 2014). Gpr1 protein is the only nutrient-sensing GPCR in yeast whereas in mammalian cells, a class of GPCRs controls the mechanisms involved nutrient sensation. Gpr1p differs from Ste2p in interacting G protein named Gpa2p, containing a long third cytoplasmic loop, and a long C terminal tails with limited sequence similarity to other GPCR classes (Xue *et al*., 1998, 2008). The protein was

discovered in two distinct ways. Firstly, Xue and colleagues isolated the C-terminus of the receptor in two hybrid screens with Gpa2, and secondly, Kraakman *et.al.* isolated a mutant with delayed glucose induced stimulation of PKA targets and found out that it had a nonsense mutation in Gpr1 (Kraakman *et al*. 1999; Xue *et al*.1998). Gpa2 is the first member of Gα family of heterotrimeric G-proteins that does not function in association with classical Gβ and Gγ subunits (Peeters *et al*., 2007). Upon glucose binding on Gpr1, the receptor triggers activation of G protein which in turn activates Cyr1, the adenylate cyclase of yeast (Figure 1.2.). Cyr1 catalyzes the synthesis of cyclic adenosine monophosphate (cAMP) from ATP. This second messenger, cAMP, is capable of binding on regulatory subunit of protein kinase A (PKA), Bcy1, and causes dissociating it from the catalytic subunits, Tpk1, Tpk2 and Tpk3, which are able to phosphorylate downstream target molecules and by this way, regulate protein activity and gene expression (Peeters and Thevelein, 2014). Gpa2 can also activate PKA through an adenylate cyclase bypass pathway. The kelch repeat proteins, Krh1 and Krh2, were identified with a structure very similar to seven-WD-40 repeat structure of Gβ proteins, and physically interacted with Gpa2 (Harashima and Heitman 2002, 2005). Krh1 and Krh2 proteins bind to the catalytic subunits of PKA and trigger their interaction with the regulatory subunit, which makes the dissociation of subunits difficult. Krh1 and Krh2 mediate the phosphorylation of Bcy1 and causes in this way production of a more stable and effective form of the protein as an inhibitor catalytic subunits (Budhwar *et al*., 2010). Thus, inactivation of the Krh proteins by Gpa2 suggests an independent pathway of adenylate cyclase activation for PKA stimulation (Lu and Hirsch, 2005; Peeters *et al*., 2006).

The PKA has regulatory effects on a vast majority of processes in yeast. It functions as a key player in control of metabolic pathways as glycolysis and gluconeogenesis, in control of growth and proliferation of the cells, in stress tolerance, in developmental pathways like pseudohyphal differentiation and sporulation, and several other pathways and processes (Santangelo, 2006; Thevelein, 2000). The general role of PKA is triggering fermentative growth while inhibition of stationary-phase characteristics and other processes depending on respiration like sporulation

(Peeters and Thevelein, 2014). Immediately after the discovery of Gpr1-Gpa2 GPCR signaling system, scientist studied on mutant yeast cells to have a better understanding the key molecule in this system. It is observed that deletion of Gpr1 is not lethal for yeast and only causes delayed activation of cAMP-PKA signaling pathway after addition of glucose (Kraakman *et al*., 1999). Although the extracellular glucose signaling through this GPCR system is solely dependent on activation of Ras by glucose catabolism in the cell, the opposite is not correct. Hence, glucose can still results in stimulation of cAMP-PKA pathway in the absence of Gpr1 or Gpa2 (Rolland *et al*., 2000). Other research on deletion studies with Gpa2 showed that Gpa2 deletion is also not lethal for yeast cells and similarly it results in delayed glucose-induced stimulation of the pathway and affects other PKA-dependent phenotypes as pseudohyphal growth (Nakafuku *et al*., 1988; Kubler *et al*., 1997). In general, deletion of Gpa2 results in stronger phenotypic effects than deletion of Gpr1, which indicates an additional regulation at Gpa2 level (Versele *et al*., 1999).

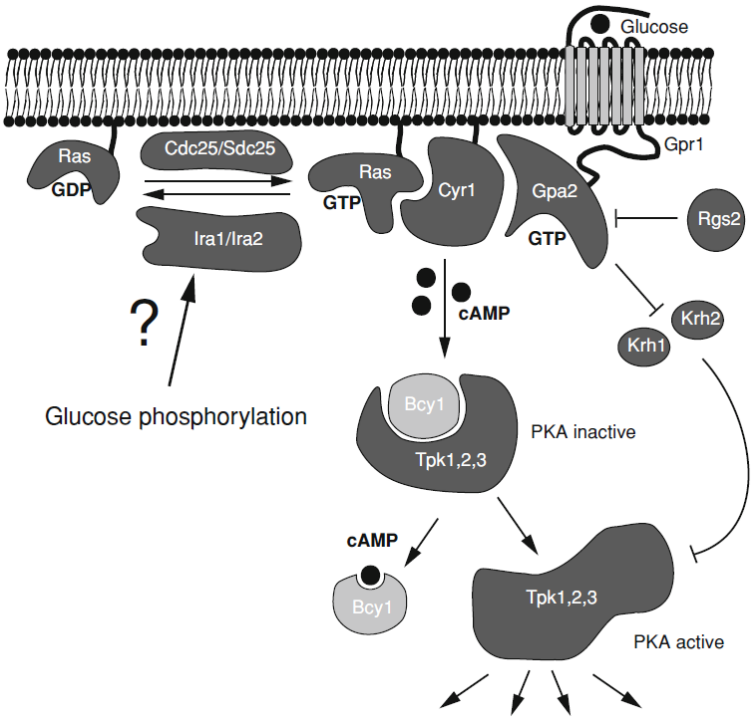

Figure1.2 Glucose activation of cAMP-PKA pathway (Peeters and Thevelein, 2014).

1.1.1.2. Ste2p, Receptor for Alpha-factor Pheromone

Haploid yeast cells secrete pheromones to signal mating, and respond these chemical factors by growing a projection towards a potential mate. Upon contact of two partner haploid yeasts, they start to fuse for production of a diploid zygote. Pheromones are the ligands of specific GPCRs expressed on cell surface of the opposite mating type and binding of the peptide to its corresponding receptor triggers activation of receptor-associated heterotrimeric G-proteins, which in turn stimulate activation of mitogen-activated protein kinase (MAPK) pathway. MAPK cascade elements mediate the expression of mating-specific genes, and in this way, control cell cycle arrest, polarized morphogenesis in the direction of the partner cell, named as shmooing, cell–cell fusion and karyogamy to produce a diploid zygote (Merlini, Dudin and Martin, 2013). There are two different pheromone factors (**a**- and **α**-factor) and GPCRs (Ste2 and Ste3) in *S.cerevisiae* for two haploid types of the organism (MAT**a** and MAT**α**). Although the receptors and their ligands differ in their final structure, they use the same action of mechanisms and downstream effector molecules to transmit the extracellular signal to the intracellular sites. In this study, we studied Ste2p in MAT**a** type of haploid yeast cells. The α-factor, pheromone produced by MAT**α** cell, binding to Ste2 promotes GDP to GTP exchange on Gα subunit, Gpa1, and allows dissociation of Gβγ complex, Ste4 and Ste18, to activate mating signaling (Figure 1.3.) (Elion, 2000). Gβ principally interacts with key effector molecules: upon dissociation of the complex, it binds to p21-activated kinase (PAK)-like kinase Ste20, the MAPK scaffold protein Ste5, the Cdc42-guanine-nucleotide exchange factor (GEF) Cdc24 and the scaffold protein Far1, which has a key role in determining the site of cell polarization during mating (Leeuw *et al*., 1998; Whiteaway *et al*., 1995; Wang *et al*., 2005).

Polarizing growth toward the partner cell is one of the consequences of mating signaling pathway in *S.cerevisiae*. Pioneer experiments in the field clearly showed that, in mating mixtures containing MAT**a** cells, and the same numbers of pheromone-producing and non-pheromone-producing MAT**α** partners, MAT**a** cells are capable of discriminating the two groups of its partners, and mate almost only

with pheromone-producing partners (Jackson and Hartwell, 1990). Nonetheless, when pheromone receptors are saturated through high concentrations of pheromone factors, individual cells get confused and mate randomly with partners from groups of either producing and non-producing cells, through the so-called 'default pathway', where the possible bud site becomes the shmoo site (Dorer, Pryciak, Hartwell, 1995; Madden and Snyder, 1992). Another important finding on mating process is the production of proteases, which cleave and inactivate pheromones, by yeast cells, hence directly remodeling the pheromone landscape in their environment (Merlini, Dudin and Martin, 2013). For instance, the alpha-factor protease Bar1, which is expressed and released by MAT**a** cells, enables these cells avoid each other (Jin *et al*., 2011; Barkai, Rose and Wingreen, 1998).

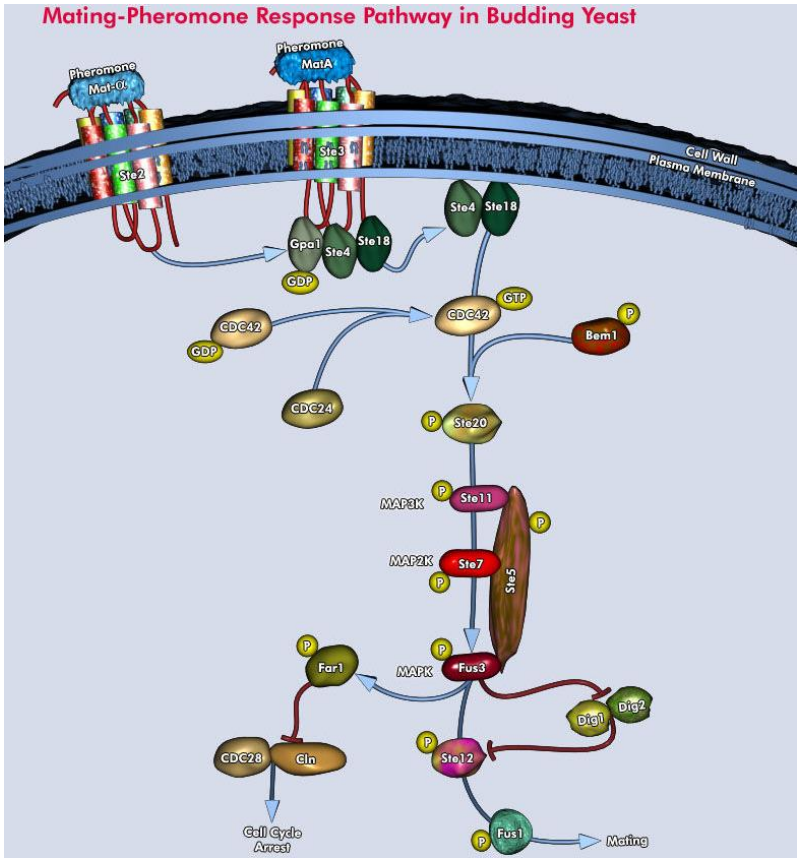

Figure1.3 Mating-Pheromone response pathway in Saccharomyces cerevisiae. (Retrieved from: http://www.qiagen.com/products/genes%20and%20pathways/pathway%20details.aspx?pwid=283)

1.2. Biogenesis and Trafficking of Yeast Membrane Proteins

Delivery of the proteins to the correct subcellular destination is a critical process, which is mainly driven by specific signals residing in the proteins themselves. The most common class of sorting signal is the one directing a protein to the secretory pathway where numerous proteins destined for the extracellular environment or retention in the internal endomembrane system are sorted. Secretory proteins enter the series of interconnected organelles at endoplasmic reticulum (ER) that governs protein translation, its translocation across the membrane, protein folding, post-translational modification and traffic of proper cargo molecules (Barlowe and Miller, 2013). Like mammalian GPCRs, yeast GPCRs are inserted into the membrane of ER, folded into their native conformations, and transported through the secretory pathway to the plasma membrane (Stefan, Overton and Blumer, 1998).

When the hydrophobic signal sequence of GPCRs is translated and recognized by the signal-recognition particle (SRP), the major pathway for delivery of nascent secretory proteins, co-translational translocation process into ER is initiated. After recognition, ribosome-nascent chain complex is targeted to Sec61 translocons through an initial interaction between SRP and ER-localized SRP receptor encoded by SRP101 and SRP102 (Ogg *et al*., 1998). In fact, deletion studies of the SRP components in yeast cells surprisingly indicate that SRP-dependent pathway is not crucial, and other cytosolic machinery manage delivery of all essential secretory proteins to the translocon (Hann et al. 1992; Stirling and Hewitt 1992). Maturation of those proteins in yeast is a result of multi-step mechanism that takes place in the ER and a prerequisite that is required to be completed before trafficking of the cargo molecules. Although in maturation steps, anterograde pathway known as forward-moving is mainly indicated, retrograde pathway balancing forward moving by returning the resident proteins carrying correct signal sequence is also a noteworthy part of trafficking of membrane proteins. Initially, signal peptidase complex (SPC) recognizes and removes N-terminal signal sequence by endoproteolytic cleavage during translocation through the Sec61 complex (Meyer and Hartmann 1997). The addition of oligosaccharides to consensus Asn-X-Ser/Thr sites in nascent

polypeptides occurs during their translocation through the Sec61 pore. Furthermore, signal sequence cleavage must take place before attachment of N-linked oligosaccharide for N-linked glycosylation sites that are near signal sequence cleavage sites (Chen *et al*. 2001). This N-linked structure is thought to be a significant part of a system that functions in protein folding and quality control to handle misfolded glycoproteins (Schwarz and Aebi, 2011). In addition to N-linked glycosylation, O-linked glycosylation occurs by the attachment of mannose on Ser/Thr residues of secretory proteins. This type of modification of those proteins is crucial in *Saccharomyces cerevisiae* since it is required for normal morphogenesis as well as cell wall integrity (Strahl-Bolsinger *et al*., 1999). Thirdly, ~15 % of secretory proteins receive a lipid-anchored glycosylphosphatidylinositol (GPI) moiety to their C terminus. GPI synthesis and attachment are important processes especially in yeast since GPI anchored proteins are thought to have significant roles in cell wall structure and cell morphology (Pittet and Conzelmann, 2007). In the literature, a couple of studies represent that proteins, which do not receive attachment of GPI anchor and removal of C-terminal hydrophobic signal, are not exported from the ER, thereby their further process is blocked in secretory pathway (Nuoffer et al. 1993). Finally, in most cases, disulfide bonds are formed in those proteins when nascent polypeptides are translocated into the oxidizing environment of the ER lumen. The most significant role of this bond formation is to facilitate correct protein folding in the ER lumen (Barlowe and Miller, 2013).

Once proteins completed their maturation in the ER, they become available for forward traffic, a process governed by an array of transport vesicles, which bud off from one compartment, pass through the cytoplasm, and fuse with a downstream compartment. ER-derived vesicles are distinguished by their COPII coat, which is responsible for creating a spherical transport vesicle from a planar donor membrane and fill the nascent vesicle with the appropriate cargoes (Barlowe *et al.*, 1994). Minimal COPII coat machinery is composed of five proteins and its assembly is triggered by the local recruitment and activation of the small G protein, Sar1 upon catalysis of exchange of GDP for GTP by an ER membrane-bound guanine nucleotide exchange factor (GEF), Sec12 (Nakano et al. 1988; d'Enfert et al. 1991).

At the end, the fully assembled coat is composed of two distinct layers: the inner membrane layer, which associates with lipid headgroups and functions in cargo binding, and the outer membrane distal layer, which forms a polymer structure that drives membrane curvature (Matsuoka *et al.,* 2001). Both layers have effects on catalytic cycle of Sar1 and enhancing maximal GTPase activity only when the coat is fully assembled (Antonny *et al.,* 2001). Selective collection of cargo in transport vesicles is thought to depend on recognition of specific sorting signals by COPII coat. Those signals vary from simple acidic peptides to folded epitopes and act either by direct interaction with the coat or by indirect way that involves binding to a cargo adaptor, which links them to the coat (Dancourt and Barlowe, 2010). Direct interactions with coat are observed in low affinity that supports the transient nature of association of cargo with the coat. Proteins must interact with the coat during vesicle formation and also be released upon vesicle fusion, thereby allowing coat recycling and exposure of fusogenic domains (Mossessova *et al.,* 2003). Moreover, in adaptor involved indirect interactions with the coat, some adaptors are observed to function as canonical receptors, which bind to their ligands in one compartment and interact with the units of the coat to couple cargo with it, then release its ligand in another compartment most probably as the result of an alteration in ionic strength or pH of the acceptor compartment (Barlowe and Miller, 2013).

After budding off COPII vesicles from ER membranes, binding and fusion machineries guide those transport vesicles to Golgi acceptor membranes. Generally, the vesicles are tethered to Golgi membranes through the action of the Ypt1 GTPase, Uso1 and transport protein particle I (TRAPPI) complex . Moreover, fusion of the vesicle to Golgi acceptor membranes is mediated by assembly of membrane-bound SNARE (soluble Nethylmaleimide-sensitive factor attachment protein receptors) protein complexes. After arrival of secretory cargo at the *cis*-Golgi, they may undergo further outer-chain carbohydrate modifications and proteolytic processing as cargo passes through Golgi compartments. N-linked core carbohydrate of glycoproteins may be extended by addition α-1,6-mannose residues in the *cis*-Golgi and by addition of a-1,2- and α-1,3-mannose residues in the medial compartment of

Golgi. Moreover, Kex2-dependent proteolytic processing of some cargo molecules takes place in *trans*-Golgi compartment (Graham and Emr 1991; Brigance et al. 2000). In *Saccharomyces cerevisiae,* unlike mammalian cells, individual golgi cisternae are observed scattered over the cytosol. Thus, a different transport model called cisternal maturation model favored in the transport of proteins through Golgi. Upon delivery membrane proteins to *cis* Golgi, individual compartments containing the cargoes form at cis-site of the organelle and, first, mature into medial, then trans compartment, thereby suggesting that vesicles are transported between distinct compartments of Golgi complex, cisternae carry the cargo proteins through the organelle (Papanikou & Glick, 2009).

In contrast to anterograde transport through Golgi compartments, the COPI coat is thought to control retrograde transport within the Golgi complex to retrieve recycling Golgi machinery to earlier compartments as Golgi cisternae mature (Bonifacino and Glick, 2004). Although the role of COPI mediated vesicular traffic within the Golgi remains controversial, their role in retrograde Golgi-ER transport is well understood (Emr *et al*., 2009). Like the COPII coat, COPI compromises two layers: inner layer for cargo binding and an outer layer. In addition to that, assembly of COPI on the membrane is also a similar process to COPII by means of initiation by a small membrane-bound GTPase, Arf1 (Antonny et al., 1997). Moreover, capturing of ER resident membrane proteins via the vesicles depends on recognition of sorting signals, mostly canocical retention motifs, K(X)KXX, which is located at the C terminus of the cargo and membrane-proximal (Shikano and Li 2003).

There are two routes suggested for final destination of membrane proteins from *trans*-Golgi to PM in *Saccharomyces cerevisiae.* First way applies for periplasmic enzymes that are transported through clathrin coat vesicles passing through endosomal compartments, and second one describes transportation of PM and GPI anchored proteins in a lipid raft dependent way (Surma, Klose, & Simons, 2012; Zabrocki *et al*., 2008). Major components of lipid raft dependent transport are ergosterols, sphingolipids and GPI anchored proteins. Upon association of cargo proteins with lipid rafts, they are targeted to transport carriers, then; raft platform is

formed by the activity of clustering agents on lipid rafts. The cytoskeletal components are thought to function in formation of membrane curvature and budding of vesicle from Golgi, however, it still remains unclear (Surma *et al.*, 2012). Eventually, the cargo molecules are trafficked to their final destination on the plasma membrane.

1.3. Dimerization and Oligomerization of G-protein coupled receptors

Many membrane, cytosolic and nuclear receptors exist and function as dimers and, in some cases, oligomers (Heldin, 1995). Dimers can form between either identical (homodimerization) and/or different (heterodimerization) proteins. At the beginning, several research groups were questioning the formation of receptor dimers. Now, since it is well accepted that many receptors form dimers and/or oligomers, the question has turned to find the reasons behind formation of receptor complexes. Results of experiments addressing to find mechanistic effects of receptor dimerization in living cells are summarized and listed in Table 1.1 (Lohse, 2010).

Table 1.1 Mechanistic effects of receptor dimerization (Lohse, 2010).

Mechanism	**Properties acquired by dimerization**
Ligand recognition	• Specificity through interactions of ligands with two subunits in a dimer • Increased affinity through multiple contact points • Increased ligand repertoire via different binding partners
Receptor activation	• Changes in distance between subunits as an activation mechanism • Cross-phosphorylation as an activation mechanism
Signal Transduction	• Multiple contact points and specificities for intracellular signaling proteins • Cross-regulation of activity in promoters
Trafficking	• Changes in cell surface delivery • Cross-regulation in receptor internalization
Cell surface mobility	• Cross-regulation in cell surface mobility

Initially, GPCRs have been classified as receptors that do not need to dimerize (Heldin, 1995). Because their heptahelical structure allows a variety of movements and rearrangements that permit transmission of the activation signal across the membrane, tightly packed structure provides ligand specificity, and anchoring of G-proteins to the intracellular site of receptors in their active form provides a straight transduction mechanism (Rosenbaum, 2009; Park *et al*., 2008; Scheerer *et al*., 2008). Additionally, recent data on β2-adrenergic, rhodopsin and μ-opioid receptors shows that GPCRs do not need to form dimers to execute their fundamental function of signal transduction from ligand to activate G-protein, hence it is suggested that the signaling of this class of receptors as monomers is possible at physiological speed (Whorton, 2007, 2008; Kuszak, 2009). However, experimental results accumulated over the past two decades indicates that they can form homomers and heteromers in living cells (Bouvier, 2001; Milligan and Bouvier, 2005; Ferré *et al*., 2009). Early evidences on the subject result from the studies as functional complementation of dysfunctional receptors, co-precipitation of separately labeled GPCRs, and dimer visualization in sodium dodecyl sulfate (SDS) - polyacrylamide gels, receptor disruption by receptor peptides and radiation inactivation (Hebert and Bouvier, 1998). The most valuable physiological evidence came from a study on $GABA_B$ receptors that revealed formation of a dimer between $GABA_{B1}$ and $GABA_{B2}$ is a requirement both for cell surface targeting and functioning. $GABA_{B1}$ can bind the agonist but cannot couple to G-protein whereas $GABA_{B2}$ cannot bind agonist but can couple to G-protein; hence, formation of dimers allows them to complement each other for proper localization and activity (Kaupmann *et al*., 1998). Later, FRET experiments using extracellularly tagged $GABA_B$-receptors showed that the receptors even form tetramers including two close $GABA_{B1}$ protomers, which probably form the center of tetramer, and two distant $GABA_{B2}$ protomers (Maurel *et al*., 2008). Now, it is agreed on, that family C GPCRs, including $GABA_B$ and calcium-sensing receptors, form important homo- or heteromers for proper functioning (Kniazeff *et al*., 2011).

After consensus on formation of dimers and higher order oligomers, the dynamics of these GPCR complexes became the center of the research on the subject. The data

from early studies on $GABA_B$ receptors and V_2-vasopressin receptors suggested that GPCR dimerization occurred early in their biosynthetic pathways. As mentioned above, for cell surface targeting of $GABA_B$ receptors, interaction of C-termini of B_1 subunit and B_2 subunit is required and the studies of V_2-vasopressin receptor mutants revealed that the receptors are observed already as dimers in the endoplasmic reticulum of living cells (Bouvier, 2001; Zhu and Wess, 1998). From these studies, it is understood that these dimers are quite static and either a very high affinity of two monomers for each other or a covalent S-S bond as observed in some class C GPCRs are required for such a static interaction. Furthermore, the consistent results of structure-function studies of diverse homo- and heterodimer class C GPCRs indicated that the region that capable of coupling to proteins is located in heptahelical domain, whereas the region responsible for formation of stable dimers and their delivery to the cell membrane resides in other parts of the receptor (Gurevich and Gurevich, 2008). In some studies, researchers tried to understand the binding mechanisms in dimer and oligomer complexes and took advantage of physical chemistry. Even for short-lived GPCRs (2-20 hr), to exist in a stable dimer, the monomers must interact with an affinity ranging from 10 to 100 pM, which require a binding energy that is achieved by covalent interactions observed in class C GPCRs (Palczewski *et al*., 2000; Li, 2004; Rasmussen, 2007).

GPCR dimers are believed to have special functions in the cell (Gurevich and Gurevich, 2008). Acting as a desensitization mechanism, which is immediate suppression of G-protein mediated signaling when the active receptors are outnumbered in the environment, is one of the major mechanism acquired by GPCR dimerization. The significant reduction of neurotensin NTS1 receptor signaling efficiency upon dimerization, and more efficient coupling of monomeric rhodopsin to transducin are the strong evidences that support the mechanism (White *et al*., 2007; Bayburt *et al*., 2007). Dimerization is also believed to play a role in the progression of newly expressed GPCRs from ER to Golgi to the plasma membrane. The facilitated transportation of two subtypes of α-adrenoceptors to cell membrane by co-expression of β_2-adrenoceptor (Prinster *et al*.,2006), and the delivery of a mutant rhodopsin lacking the targeting sequence to the outer segment only with wild-

type rhodopsin are consistent with this idea (Concepcion, 2002). Additionally, several studies recently showed cross-phosphorylation and β-arrestin-mediated cross-internalization of receptor heterodimers (Abdalla *et al*., 1999; Pfeiffer *et al*., 2002, 2003; Breit, Lagace and Bouvier, 2004). In an elegant study, heterodimerization of cyclophilins fused to β-arrestin 2 and V1a and V2 vasopressin receptors, respectively, was promoted via a synthetic bivalent dimerizing agent, and it is showed that binding of β-arrestins to either of the two receptors is clearly sufficient to induce co-internalization of both when the agonist-mediated receptor activation is completely absent (Terrillon and Bouvier, 2004).

1.3.1. Methods to detect dimerization of G-protein coupled receptors

There are more than one way to show the formation of GPCR dimers in living cells. After the existence of GPCRs as homomers and heteromers became widely accepted, an explosion of data supporting this idea has accumulated and stored in Database of GPCR-GPCR Interactions (http://bioserver.ceng.metu.edu.tr/IntGPCR/about.php) (Khelashvili *et al*., 2010). The data collection is continuously enriched by the results of experiments using biophysical methods such as bioluminescence and fluorescence resonance energy transfer (BRET and FRET, respectively), fluorescence complementation, co-immunoprecipitation or combination of these distinct techniques (Milligan and Bouvier, 2005; Ferré *et al*., 2009).

Each individual technique has some limitations for specific conditions which create the variety in methods used to detect GPCR dimers. In an early study, Hebert and his colleagues co-expressed c-myc- and HA-tagged β2-adrenoceptors in application of co-immunoprecipitation method to observe β2-adrenoceptor dimers in insect cells (Hebert *et al*., 1996). In another early study, FRET method (explained briefly in the following part) was applied to reveal homodimers of yeast GPCR, Ste2p, and their location in living cells (Overton and Blumer, 2000). Later, the method was applied on gonadotropin releasing hormone (GnRH) in a different context to observe a dose-dependent increase in FRET signal, which indicates increase in dimer formation, upon agonist addition to the culture media (Cornea, Janovick, Maya-Nunez and Conn, 2001). As an alternative to FRET, BRET, the technique in which energy

transfer from luciferase oxidated substrate to a fluorescent protein occurs, also used in several studies for detection of GPCR dimers in intact cells (Milligan, 2004). BRET was used to show homodimerization of melatonin receptor 1 and 2, for the first time, and homodimerization of β2-adrenergic receptors as well (Ayoub *et al*., 2002; Angers *et al*., 2002). Functional complementation assays, which are explained in detail in the following part, are another way applied to observe GPCR dimers in cellular systems. With the advancement in technology and requirement of more efficient and definite reporter systems, apart from dimerization studies searching for new dimers, there are many studies on optimization of several techniques for detection of interacting complexes under completely different conditions.

1.3.1.1. Förster (Fluorescence) Resonance Energy Transfer (FRET)

The complete understanding of any cell biological process needs its non-destructive observation and evaluation in living cells. FRET techniques individually suitable to overcome this challenge and also make it possible to study cellular mechanisms in intact live organisms (Hasan *et al*., 2004). Moreover, FRET biosensors are also applicable in many *in vitro* formats ranging from single molecule assays to ultra-high throughput screening. In past few years, a couple of technological advances have made the design and application of FRET biosensors easier. In fact, most importantly, the rapid expansion of palette of fluorescent proteins (FPs) and advances in their properties facilitated the establishment of many new FRET biosensors (Giepman, Adams, Ellisman and Tsien, 2006; Tsien, 2006; Shaner *et al*., 2008).

FRET applies two fluorophores, a donor and an acceptor, of which the emission spectrum of donor overlaps with the absorption spectrum of acceptor. If two fluorophores are spatially located, donor excitation results in only donor emission with high efficiency. However, if they are located in close proximity (1-10 nm), excitation of donor results in emission of acceptor due to overlap in their spectra that permits resonance energy transfer from donor to acceptor molecule. The technique is now commonly applied specifically in the context of cellular signaling to reveal

interactions as the formation of protein complexes, and to figure out molecular dynamics such as alterations in protein conformation. Combination of FRET with fluorescence and laser scanning confocal microscopy applications simultaneously provides the information about the location within a single cell in which the expected interaction takes place in two and three dimensions (Hayward, Goguen and Leong, 2010).

Although no light photons (or fluorescence) are transferred to the acceptor, using the term 'fluorescence' in the name causes misleading about the phenomenon. Hence, in many studies, the name of the process is mentioned as Förster resonance energy transfer after the pioneering German physicist Theodore Förster who principally described the process many years ago (Förster, 1948). The distance at which the probability of the energy transfer from donor molecule to acceptor molecule is 50% is named as Förster distance, R_0 that depends on the spectral overlap of fluorophores, the orientation of electric dipoles, refractive index of the media and on the quantum yield of the donor fluorophore (Lakowicz, 2006). Under standard conditions, the R_0 is defined as a characteristic property of each donor-acceptor pair as a group of molecules (Kalab and Soderholm, 2010). The efficiency of FRET (E) depends on two factors: R_0 and the distance R between donor and acceptor, and calculated by the following formula $E = \frac{1}{1+(\frac{R}{R0})^6}$ (Förster, 1948).

As mentioned before, detection range of FRET varies between 1-10 nm which makes working on most biological molecules and complexes when their sizes are considered. In particular, the range of distance for sensitive FRET measurements were calculated as ~ 0.5–1.5 R_0, corresponding to ~3–8 nm in the case of the CFP-YFP pair. This range can be minimized in small molecule donor-acceptor pairs with very short R_0 as short as 1 nm (Sahoo, 2006).

FRET sensors designed to be used both *in vivo* and *in vitro* are certainly advantageous but production of such versatile sensors cannot be easy and is not always required in every single case. For instance, a FRET sensor, which is suitable for *in vitro* applications, may have toxic effects when introduced into cells, and similarly, a well-established cell-expressed FRET sensor may be difficult to isolate for large scale *in vitro* assays (Kalab, 2006, 2008).

One of the important steps in design of FRET experiment is the choice of fluorophores. The most commonly used donor-acceptor pairs in biological applications are synthetic organic dyes and fluorescent proteins in addition to the intrinsically fluorescent natural amino acids (Giepmans, Adams, Ellisman and Tsien, 2006; Tsien, 2006). The main advantages of synthetic organic fluorophores are their small size as small as less than 1 kDa and their favorable spectral and photochemical properties compared to fluorescent proteins (Roy, Hohng, Ha, 2008). In contrast, FPs are significantly larger (~25-30 kDa) and some members have sub-optimal photochemical and/or spectral characteristics which seems to be drawbacks of them in applications. However, the genetic control of this class of sensors easily cancels out such drawbacks. Moreover, there are still ongoing research for improvement of FPs, hence the performance of current FRET sensors can be increased by using the new donor-acceptor pairs (Giepmans, Adams, Ellisman and Tsien, 2006; Tsien, 2006). The high molecular photostability and brightness under continuous illumination are the most definitive properties of FRET pairs and it should be considered that in some FPs, the high brightness is not correlated with photostability (Shaner *et al*., 2008). Like in other methods using the emission from both donor and acceptor, the brightness of donor and acceptor molecules need to be in similar range to eliminate the possible problems originating from limited detection range of the instruments. For exactly the same reasons, the difference between concentrations of the donor and acceptor molecules in the sample should not be more than 10-fold (Piston and Kremers, 2007). The choice of the sensor with long excitation and emission spectra causes increased light penetration into the sample and results in less cellular damage by ultraviolet excitation. The photodamage of cells interferes with the visualization of normal function, and often stimulates rise of cellular autofluorescence (Kalab and Soderholm, 2010).

Because of its brightness, photostability and monoexponential fluorescence lifetime, enhanced green fluorescent protein (EGFP) is a distinguished donor for the detection of FRET. Hence, the study using EGFP-mCherry and EGFP-mRFP as FRET pairs for high resolution FLIM-FRET imaging in neurons clearly demonstrated the success

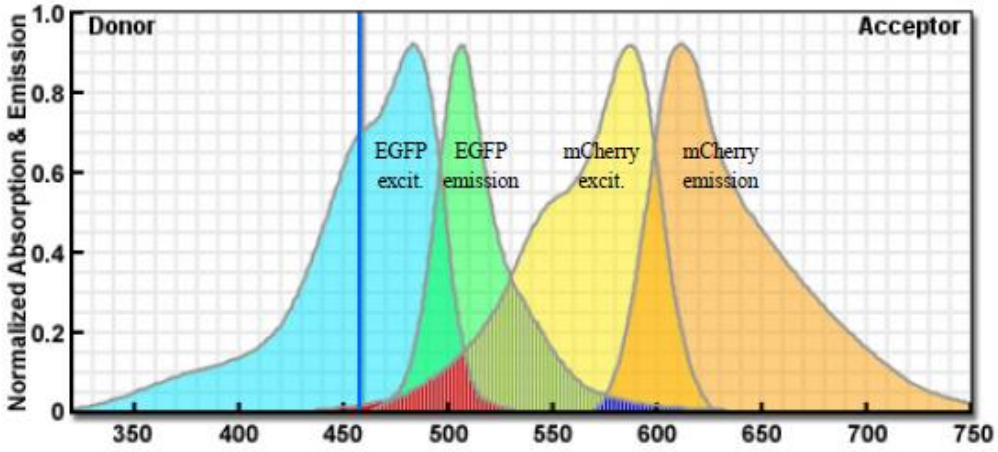

Figure 1.4 Spectral characteristics of EGFP and mCherry (JAVA tutorial of Microscopy of Nikon®)

of these FRET pairs (Yasuda *et al*., 2006). Data from a later study support the success of EGFP-mCherry couple as a FRET pair by nicely representing the spectral overlap and low level of crosstalk between excitation and emission spectra of EGFP and mCherry (Figure 1.4) (Albertazzi, Arosio, Marchetti, Ricci and Beltram, 2009).

1.3.1.2. Bimolecular Fluorescence Complementation (BiFC)

Protein complementation assays are recent methods for studying protein-protein interactions although the reassembly of protein fragments was observed over 60 years ago in the studies of ribonuclease and beta-galactosidase (Richards, 1958; Ullman, Jacob, Monod, 1967). In fact, conditional reassembly of split proteins was firstly demonstrated with a study in which inactive ubiquitin fragments were attached to interacting protein pairs, thus, interaction resulted in increased local concentration of protein fragments and enabled the conditional reassembly of split fragments (Johnson and Varshavsky, 1994). Since this study provided a direct method to link the non-covalent interaction of two proteins to the function of split reporter protein, it was a pioneer of development of the several other split-reporter assays (Shekhawat

and Ghosh, 2011). Split-protein pairs that are now commonly used are listed as: green fluorescent protein (GFP) and its variants (Ghosh, Hamilton and Regan, 2000; Hu and Kerppola, 2003), dihydrofolate reductase (DHFR) (Pelletier, Campbell-Valois and Michnick, 1998) , β-lactamase (Galarneau, Primeau, Trudeau, Michnick, 2002) , firefly and other luciferases (Luker *et al*., 2004; Remy and Michnick, 2006; Paulmurugan and Gambhir, 2003), tobacco etch virus (TEV) protease (Wehr *et al*., 2006), and thymidine kinase (Massoud, 2010).

For a successful split-reporter protein system, there are a few criteria that the characteristics of split fragments must be met. First of all, individual split fragments should not exhibit any activity, and in that point, the affinity of the fragments in the absence of attached interacting proteins should be negligible. Secondly, reassembled, active reporter protein must give an easily detectable and measurable read out. In principle, most proteins can be split into such fragments; however, the idea is not practical in every case. The limitation of the method is the identification of appropriate dissection sites within a protein that matches the criteria for use in the split protein assays.

When a fluorescent molecule is used as a reporter in this assay system, then it is called bimolecular fluorescence complementation. This specific type of split-reporter system is now commonly used not only *in vivo* protein-protein interaction studies but also monitoring the effects of extracellular agents as drugs or agonists on protein complexes *in vivo* (Morell, Ventura and Aviles, 2009). The advantage of this method is also emphasized in a study using split-EGFP as a reporter of the interested protein-protein interactions in *Saccharomyces cerevisiae.* In the study, split-EGFP fragments, so called N-EGFP and C-EGFP, were used to label phosphofructokinase subunits, Pfk1 and Pfk2. Upon interaction of two subunits, a detectable green signal was acquired from the cytoplasm. Hence, the system did not only confirm the interaction but also enable the scientists to detect the localization of it (Barnard *et al*., 2008).

1.4. Aim of the study

From the discovery, many members of GPCR classes were shown to be located on cell membrane and transmit the extracellular signals to intracellular sites as monomeric units. In contrast, experimental results in last twenty years clearly demonstrated that some of them found, function and transported in dimer form. Since GPCRs are major drug targets for development of specific treatments in pharmaceutical industry, it is important to understand why these receptors need to form such complexes, where they are found and show activity in eukaryotic cells. In several evolution studies, it is shown that main proteins involved in vital processes including nutrient sensing and mating pathways of eukaryotic cells are highly conserved. Compared to multicellular eukaryotic systems, *Saccharomyces cerevisiae* is easier to study on downstream effector molecules and overall action mechanisms on the eukaryotic cell. The aim of the study is to analyze the interactions of Gpr1 proteins in live yeast cells and we hypothesized that:

- Gpr1 proteins only exist as homodimers on the cell membrane where they show their major activity,
- Gpr1-Ste2 heterodimers are only formed on plasma membrane due to close relation between nutrient sensing and pheromone signaling pathways.

CHAPTER 2

MATERIALS & METHODS

2.1 Materials

2.1.1. Yeast strains, Culture Media and Conditions

Saccharomyces cerevisiae strains W303-1A (*MAT***a** *leu2-3,112 trp1-1 can1-100 ura3-1 ade2-1 his3-11, 15* GAL SUC2 HIS3 LEU2 ADE2 URA TRP), LK5 (*MAT***a** *leu2-3,112 trp1-1 can1-100 ura3-1 ade2-1 his3-11, 15* gpr1 Δ::LEU2), and DK102 (*MAT***a** ura3-52 lys2-801am ade2-101oc trp1-Δ63 his3-Δ200 leu2-Δ1 ste2::HIS3 sst1-Δ5) transformed with expression vectors carrying fluorescent protein tagged receptors were used throughout the study (Kraakman *et al.*, 1999; Dohlman, Goldsmith, Spiegel and Thorner, 1993). First two strains were kindly provided by Prof. Johan Thevelein from Katholieke University of Leuven, Flanders, Belgium, whereas the third was from Prof. Dr. Jeffrey Becker from University of Tennessee, Knoxville, USA.

In this study, four different culture media named as yeast extract-peptone-dextrose (YEPD), medium lacking tryptophan (MLT), medium lacking uracil (MLU) and medium lacking tryptophan and uracil (MLTU) were used for growth and maintenance of yeast strains. For yeast transformation experiments, *S. cerevisiae* W303-1A and LK5 cells were grown in YEPD liquid medium at 30°C in a shaking incubator (Zhiheng) at 200 rpm overnight. Furthermore, the other three media, MLT, MLU and MLTU were used as selection tool in those studies. Yeast cells transformed with plasmids were incubated at 30°C for 2-3 days.

The yeast strains were maintained on corresponding type of solid medium at 4°C for short term storage purpose. In order to prepare long term stocks maintained at

-80 °C, 87% (w/V) glycerol was mixed with aliquot of culture until the final glycerol concentration was 15% (V/V).

All these media were prepared by dissolving their ingredients in distilled water and sterilized by autoclaving at 121°C for 20 minutes (Appendix F,G).

2.1.2. Bacterial Strain, Culture Media and Conditions

Escherichia coli TOP10 strain was used for amplification of the prepared plasmids in this study. LB liquid and solid media were used to grow bacterial cells at 37°C for 14-16 hours in a shaker incubator (Zhiheng) at 200 rpm or an incubator (Nüve), respectively. To prepare the medium, all ingredients were dissolved in distilled water, the pH of the solution was adjusted to 7.0, and then, the medium was sterilized by autoclaving at 121°C for 20 minutes. For selection purposes of bacterial transformants, 100 μg/mL ampicillin was added to LB medium. *E. coli* cells were maintained on LB ampicillin agar plates at 4 °C for a short time and for long term storage, 15% (V/V) glycerol stocks of the cells were prepared and stored at – 80°C.

2.1.3. Cloning vectors

GPR1 gene was purchased in pBY011 parental vector from Harvard Medical School (MA, USA). The vectors carrying Enhanced Green Fluorescent Protein (EGFP), pEGFP-N2, and mCherry cDNA were kindly provided by Prof. Henry Lester of California Institute of Technology (CA, USA). All prepared constructs were cloned into either p424 or p426 bacteria-yeast shuttle vectors, which were gifts of Prof. Dr. Jeffrey M. Becker, University of Tennessee Knoxville, USA.

2.1.4. Other materials

The chemicals used throughout the study were products of Sigma-Aldrich Co. (NY, USA), Merck (Darmstadt, Germany), Applichem (Darmstadt, Germany). All restriction enzymes and One Taq Polymerase were purchased from New England Biolabs (Hertfordshire, UK). Phire Hot Start II DNA Polymerase and T4 DNA ligase were from Fermentas, Thermo Fisher Scientific (CA, USA). Oligonucleotides were synthesized by Integrated DNA Technologies (Iowa, USA) or Alpha DNA (Quebec,

Canada). Gel extraction kit was purchased from QIAGEN (Düsseldorf, Germany) whereas plasmid isolation and PCR purification kits were from Thermo Fisher Scientific (CA, USA). cAMP measurement assay kit was purchased from GE Healthcare (Buckinghamshire, UK).

Zeiss 510 laser scanning microscope at National Nanotechnology Research Center (UNAM) and Leica DMI 4000 fluorescence microscope at Biology Department of Middle East Technical University were used for imaging studies of living cells in this study.

2.2. Methods

2.2.1. Preparation of Competent *E. coli* Cells by $CaCl_2$ Method

A single colony taken from the Top 10 *E.coli* streak plate was inoculated into 5 mL of liquid LB medium in 15 ml glass tube under aseptic conditions and incubated for 12-16 hours at 37°C, 200 rpm. The culture was transferred in 50 mL of fresh LB broth in an autoclaved 250 mL flask and then incubated at 200 rpm and 37°C for 2-3 hours (OD600 should be around 0.5 to terminate the incubation period). After this time period, the *E.coli* culture at the required OD600 value was transferred to a 50 mL falcon tube and chilled on ice for 15 minutes. Later, it was centrifuged at 4000 rpm (Nüve 1200R) for 10 minutes at 4°C. After the supernatant was discarded, the pellet was re-suspended with 15 mL of sterile 0.1 M $CaCl_2$ solution. This cell mixture was kept on ice for 15 minutes, and then, centrifuged again at 4000 rpm for 10 minutes at 4°C. Supernatant was decanted and pellet was re-suspended in 4 mL of sterile, ice cold $CaCl_2$-15 % (v/v) glycerol solution. As a final step, the suspension was divided in 100 µL aliquots in 1.5 mL eppendorf tubes under aseptic conditions and immediately frozen in liquid nitrogen. This newly prepared competent *E.coli* cells were stored at -80°C.

2.2.2. Transformation of plasmids into competent *E. coli* cells

Previously prepared competent *E.coli* cells were taken from – 80°C and thawed on ice for 15 minutes. Next, 50-100 ng of plasmid DNA or 10 µL of ice cold ligation mix was added onto cell suspension and kept on ice for 30 minutes. Then, the cells

were heat shocked at 42°C for 90 seconds and chilled on ice for 5 minutes. 900 µL of LB medium was added onto the cell suspension and the bacterial cells were incubated at 37°C, 200 rpm for 1 hour. At the end of this incubation period, the cells were centrifuged at 6000 rpm for 4 minutes. 800 µL of the supernatant was discarded with the help of micropipette and the pellet was re-suspended by pipetting in the remaining supernatant. Finally, 100 µL of this cell suspension was spreaded onto LB agar plate with ampicillin. The plates were incubated at 37°C for 12-16 hours.

2.2.3. Plasmid Isolation from *E. coli* cells

A single colony was taken from agar plate and inoculated into 3 mL of LB medium with 100 µg/mL ampicillin in order to screen the recombinants or amplify the interested plasmids. The bacterial culture was incubated at 200 rpm and 37°C for 12-16 hours. At the end of incubation time, plasmids were isolated from the culture by using Thermo Scientific® GeneJET Plasmid Miniprep Kit following the user's manual.

2.2.4. Restriction Enzyme Digestion

Both single and double digestion reactions with restrictions enzymes were prepared following the instructions suggested by New England Biolabs.

2.2.5. Ligation

Digested products and plasmids were ligated *in vitro* using T4 DNA Ligase (Thermo Scientific®). The ligation mixes were prepared following the instructions of the company and the amounts of vector and insert were calculated considering their size and molar ratio as 1:5.

2.2.6. Cloning strategy for labeling Gpr1 receptors

In this study, Gpr1 proteins were tagged from two different sites: 2562^{th} base position and C-terminus. In order to insert sequences of split and full length versions of fluorescent proteins, Polymerase Chain Reaction (PCR) and Overlap Extension PCR Cloning methods (Bryksin and Matsumura, 2010) were applied.

2.2.7. Polymerase Chain Reaction

First of all, in order to transfer GPR1 gene from pBY011 vector into p424 and p426 expression vectors, two primer sets (including forward and reverse primers) were designed to generate *BamHI* and *EcoRI* restriction sites at 5' and 3' ends of GPR1 gene, respectively. Moreover, one set was specifically designed to remove the stop codon at the end of gene while inserting the cut sites. The optimized PCR mix and thermocycling conditions were as below:

Table 2.1 Optimized PCR mixtures for addition of cut sites at the ends of GPR1

Reagent	**Volume/Amount**
5x Phire Reaction Buffer	10 μL
Phire Hot Start II DNA Polymerase	1 μL
dNTP (25 mM)	0,5 μL
Forward Primer (Gpr1BamHI-F) (20 mM)	1 μL
Reverse Primer (Gpr1EcoRI-R) (20 mM)	1 μL
Template DNA (GPR1)	150 ng
Nuclease free water	up to 50 μL

Table 2.2 Optimized PCR conditions for addition of cut sites at the ends of GPR1

Cycle step	**Temperature**	**Time**	
Initial Denaturation	98°C	30 sec	
Denaturation	98°C	5 sec	**x 35 cycles**
Annealing	52.4°C	5 sec	
Extension	72°C	1 min	
Final Extension	72°C	1 min	
Hold	4°C	∞	

For insertion of the individual sequences of EGFP, mCherry and their split fragments into 2562th base position, those sequences were amplified by primers designed to

have approximately 30 bp-long overhanging regions of the insertion site of the receptor gene. The optimized PCR mix and thermocycling conditions were as below:

Table 2.3 Optimized PCR conditions for addition of flanking ends at the ends of FPs

Cycle step	**Temperature**	**Time**	
Initial Denaturation	98°C	30 sec	
Denaturation	98°C	5 sec	**x 35 cycles**
Annealing	54°C	5 sec	
Extension	72°C	1 min	
Final Extension	72°C	1 min	
Hold	4°C	∞	

In order to tag Gpr1 receptors at C-terminus, primarily, the individual sequences of EGFP, mCherry and their split fragments were amplified by using primer sets (including forward and reverse primers) designed to generate SalI and XhoI restriction sites at 5' and 3' ends, respectively. The optimized PCR mix and thermocycling conditions were as below:

Table 2.4 Optimized PCR mixtures for addition of cut sites at the ends of FPs

Reagent	**Volume/Amount**
5x One Taq Std Reaction Buffer	10 µL
One Taq DNA Polymerase	0.5 µL
dNTP (25 mM)	1 µL
Forward Primer (20 mM)	1 µL
Reverse Primer (20 mM)	1 µL
Template DNA (EGFP or mCherry)	150 ng
Nuclease free water	up to 50 µL

Table 2.5 Optimized PCR conditions for addition of cut sites at the ends of FPs

Cycle step	Temperature	Time	
Initial Denaturation	94°C	30 sec	
Denaturation	94°C	20 sec	**x 30 cycles**
Annealing	55.3°C	50 sec	
Extension	68°C	1 min	
Final Extension	68°C	5 min	
Hold	4°C	∞	

2.2.8. Agarose gel electrophoresis

Agarose gel electrophoresis was used to control the sizes of DNA fragments which were PCR or digestion reaction products. The concentration of agarose gel (w/v) was calculated depending on the size of the products. For the products that have the size between 200-3000 bp, 1.5 % (w/v) agarose gel was prepared; on the other hand, 0.8 % (w/v) agarose gel was used for the products longer than 3000bp. The gel was prepared by dissolving the specified amount of agarose in 1 X TBE in a microwave oven. After the solution cooled down for a while, EtBr was added into the solution to make DNA bands visible under UV light. DNA samples were loaded in the wells on the gel after mixed with 6 X loading dye (Fermentas®, Cat#R0611). To determine the sizes of samples, GeneRuler^{TM} 1 kb DNA Ladder and 100 bp plus DNA Ladder (Fermentas) were also run on the gel as well. The agarose gels, which run at 100 V, were visualized via Vilber Lourmat Gel Imaging System.

2.2.9. DNA Extraction from Agarose Gel

Interested DNA bands controlled on agarose gel were extracted from the gel using QIAGEN® Gel Extraction Kit (Cat#28704) by following the user manual.

2.2.10. Determination of DNA Amount

NanoDrop 2000 spectrophotometer (Thermo Scientific®) was used to detect the concentration of nucleic acids. 1.0 μL of sample DNA was loaded onto micro-volume pedestal and measured using the software.

2.2.11. Overlap Extension PCR Cloning Method

This technique includes two successive PCRs in which the product of first PCR is used as primer in the second reaction. In first reaction, the gene of fluorescent protein was amplified with 30-bp long overhangs that were homologous to determined integration site within the receptor gene. Furthermore, in second PCR, 1:5 template (plasmid carrying the receptor gene) to insert (first PCR product) molar ratio was used and at the end, the whole plasmid carrying its new insert was amplified.

Table 2.6 Optimized PCR mixtures to amplify FP tagged GPR1 by overlap extension PCR method

Reagent	**Volume/Amount**
5x Phire Reaction Buffer	10 µL
Phire Hot Start II DNA Polymerase	1 µL
dNTP (25 mM)	1µL
First PCR product	250 ng
Template DNA	50 ng
Nuclease free water	up to 50 µL

Table 2.7 Optimized PCR conditions to amplify FP tagged GPR1 by overlap extension PCR method

Cycle step	**Temperature**	**Time**	
Initial Denaturation	98°C	30 sec	
Denaturation	95°C	30 sec	**x 18 cycles**
Annealing	51°C	1 min	
Extension	68°C	23 min	
Hold	4°C	∞	

2.2.12. DpnI digestion

DpnI (Thermo Scientific Cat# ER1701) restriction enzyme recognizes N6-methyladenine within its recognition sequence, GATC. Since PCR-amplified products do not have methylated adenine at the recognition site of this enzyme, after second PCR, the products were treated with DpnI restriction enzyme following the manufacturer's instructions to digest the plasmids that were not the products of PCR.

2.2.13. Sequencing

The sequences of the genetically engineered constructs in the study were controlled by DNA sequencing. For this confirmation step, DNA sequencing service of MCLAB (California, USA) and Genoks (Ankara, Turkey) was used.

2.2.14. Super Protocol GIETZ Yeast Transformation

Super protocol GIETZ yeast transformation method (Gietz, St Jean, Woods, & Schiestl, 1992) was used to introduce prepared plasmid constructs into *S.cerevisiae* strains. First of all, yeast cells were inoculated into 3 mL of appropriate rich or selective liquid medium and incubated at 30°C and 200 rpm for 14-16 hours. On following day, 1.5 mL of yeast culture was transferred into 50 mL of fresh medium and incubated at same conditions until OD600 reached 1.0. Then, the culture was taken into a sterile falcon tube and centrifuged for 5 minutes at 3000 rpm. After the supernatant was decanted, the pellet was re-suspended in 1 ml 0.1M LiAc by gently pipetting and transferred into an eppendorf tube. The cells were centrifuged 2 minutes at 3000 rpm. The supernatant was removed and the pellet was re-suspended in 0.1M LiAc that the amount depending on the number of planned transformations. For instance, the maximum volume was 500µl and was enough for 10 transformations. After re-suspension, the following solutions were pipetted in new eppendorf tubes:

-50 µL of cells

- 300 µL Pli mix (1ml LiAc, 1 ml H2O, 8 ml 3350 PEG 50% w/V)
- 5 µL SSDNA (10mg/ml)
- 1µg plasmid DNA

In order to mix the solutions, the tubes were vortexed for 10 seconds and incubated 30 minutes at 42 °C in shaking water bath. At the end of incubation time, the cells were centrifuged 4 minutes at 4000 rpm. After the supernatant was removed, the pellet was re-suspended in 500 µL sterile water by gently pipetting and they were plated out on selective medium. The plates were incubated at 30°C for 2-3 days. On third day, 4 colonies from each plate were streaked on the appropriate selective medium for further experiments. All required solutions were either filter or heat sterilized before use.

2.2.15. Cyclic Adenosine Monophosphate (cAMP) measurement assay

This assay was used to check the functionality of introduced Gpr1 proteins labeled with fluorescent proteins by comparison of the functionality of the receptors in wild type *S.cerevisiae*. This test was composed of four parts: collecting the cells, taking the samples purification and neutralization of the samples and the measurement.

- **Collecting the cells**

On first day, a single colony from each yeast culture was inoculated in 3 mL YPD and incubated at 200 rpm and 30°C for 16 hours. After this incubation period, each yeast culture was transferred into 50 mL YPD and incubated again at the same conditions. On the following day, OD600 of each culture was measured and then, the dilution calculation was made to get a final value as 0.05 in 1 L YPD 3.5% (v/v) Glycerol medium. The cultures were incubated at 200 rpm and 30°C for 12-16 hours. This incubation time was ended when OD600 of each individual culture reached up to ~ 3-4. Next, the cultures were quickly cooled down on ice for 20 minutes. They were transferred into sterile large brown pots and centrifuged 5 minutes at 3000 rpm without brake. The supernatant was removed; the cells were re-suspended in 50 mL MES medium and transferred in pre-weighed falcon tubes. The yeast cultures were centrifuged 5 minutes at 4°C and 3000 rpm. The supernatant was removed again and the tubes were dried with paper. Afterwards, 900 mg of cells were weighed in dry 100 mL Erlenmeyer flasks and re-suspended in 24 mL MES medium.

- **Taking the samples**

One plastic tube with 10 mL 60 % methanol for every sample was previously prepared, labeled according to time points indicated below and put in ethanol bath at -40°C. Next, 1 L of 5 mM Glucose solution was prepared to trigger the pathway. Firstly, 2 mL from each sample was taken as blank. Then, upon addition of 5 mL glucose solution on individual yeast culture, 2.5 mL of samples from the flasks was transferred into the corresponding tubes with methanol at the following time points: 15 sec, 30 sec, 45 sec, 1 min, 1min 15 sec, 1 min 30sec, 2 min, 3 min. The sample tubes were centrifuged 5 minutes at 3000 rpm and -20°C. After the supernatant was collected in a flask, the tubes were centrifuged again at the same conditions. The remaining supernatant was removed with vacuum pump and the samples were chilled on ice for 5 minutes. Finally, the cells were re-suspended in 0.5 mL of perchloric acid.

- **Purification and neutralization of the samples**

The cells were transferred in 2 mL eppendorf tubes that were previously half-filled with glass pearls in advance, and homogenized in FastPrep®-24 Instrument in 20 seconds at speed 6 by repeating the step twice. Then, 0.4 mL of perchloric acid was added onto the cells and mixed by vortex. The cells were centrifuged 5 minutes at 4°C and 13 000 rpm. 250 µl of the supernatant in each tube was transferred to clean eppendorf tubes on ice. 10 µl of thymol blue (250 µg/ml stock solution) and 50 µl of 5 M potassium carbonate were added to the tubes, respectively. Afterwards, they were left on ice for 15 minutes. They were centrifuged 2 minutes at 4°C and 13 000 rpm. 200 µl of the supernatant in each tube was transferred to clean eppendorf tubes and 100 µl of 1 M HCl solution was added on them. After 10 µl of 2 M Tris buffer at 7.5 pH was added in the tubes and mixed well with vortex, the color of the solutions in each tube was checked and compared. At the end of this protocol, the expected color for neutral solution was a visible yellow color. Finally, the neutralized samples were kept at -20°C up to a couple of weeks before use.

- **cAMP measurement kit**

Amersham cAMP Biotrak Enzymeimmunoassay (EIA) System of GE Healthcare was used to measure cAMP levels in previously prepared yeast cells.

2.2.16. Imaging with Fluorescence and Laser Scanning Confocal Microscope

A single colony from streak plate was inoculated in 3 mL of appropriate liquid medium and incubated at 30°C and 200 rpm for 14-16 hours. At the end of incubation period, 1 mL of the cells were transferred into 3 mL of fresh medium and incubated at same conditions for 5 hours. In order to prevent active movement of yeast cells during imaging sessions, cells were centrifuged at 4000 rpm for 2 min and the pellet was re-suspended in 1 mL of 0.4 % agar containing MLTU medium. Finally, live *S. cerevisiae* cells were examined with Leica DMI 4000 fluorescence microscope HCX APO U-V-I 100.0 x 1.30 oil immersion objective and Zeiss LSM 510 confocal microscope with an objective Plan-Apochromat 63x/1.40 Oil DIC M27.

2.2.17. Data and Image Analysis

CLC Genomics Workbench v7.0 was used for sequence analysis of the constructs. Additionally, GraphPad Software was used in the statistical analysis of growth rate, cAMP measurement and FRET efficiency data sets.

Finally, the images taken via the camera and software system of Zeiss LSM 510 confocal microscope were processed using software named ImageJ v1.46. The FRET image processes and calculations were done via a plug-in of the program, PixFRET.

CHAPTER 3

RESULTS & DISCUSSION

3.1. Cloning of GPR1 coding sequence from PBY011 Gateway expression vector to p424 and p426 expression vectors

First of all, coding sequence (cDNA) of Gpr1 was transferred into p424 and p426 yeast expression vectors which differ mainly in their auxotrophic marker gene (Appendix C). Since the multiple cloning sites of both vectors are same, it was easy to choose two cut sites, *BamHI* and *EcoRI*, to insert the gene of interest. At the beginning, we aimed to tag Gpr1 from two different sites: 854th position and carboxy (C) - terminus. For the first position, we need stop codon at the end of the gene whereas remove it for C-terminus tagging. So primers were designed to insert *BamHI*, GGATCC, and *EcoRI*, GAATTC, sequences to 5' and 3' ends of the gene, respectively, and remove the stop codon at 3' end (Appendix B).

Using the optimized PCR conditions and mixtures for Phire II HS enzyme listed in *Chapter 2*, GPR1 was amplified with the cut sites at the ends.

Gpr1 coding sequence is composed of 2883 bp without stop codon, thus, the expected size of PCR product is ~ 2900 bp and was controlled by 1% agarose gel run at 100 V (Figure 3.1). Then, DNA fragments with the correct sizes were extracted and purified from the gel using gel extraction kit.

PCR products in correct size that indicated in red boxes were excised from agarose gel, and these products, p424 and p426 vectors were digested with *BamHI* and *EcoRI* restriction enzymes in separate tubes. Digested GPR1 products were purified by PCR purification kit. In contrast, digested vectors were run on 0.8 % agarose gel (Figure 3.2) and the band with correct size (shown in red boxes) extracted from the gel.

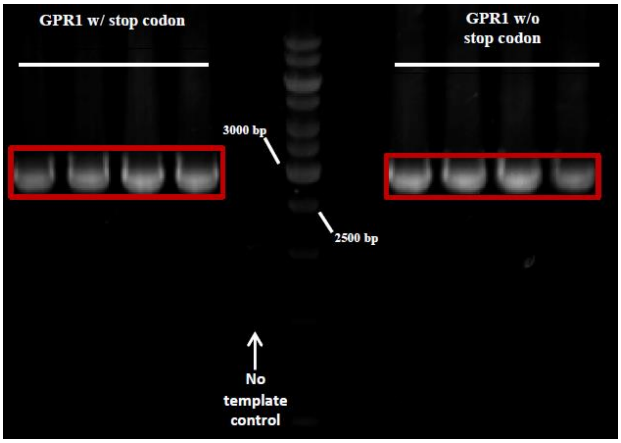

Figure 3.1 PCR products of cut site addition at the ends of GPR1 shown in red boxes. Lane 1-4: GPR1 with stop codon. Lane 5: No template control. Lane 6: Gene Ruler 1 kb DNA Ladder. Lane 8-11: GPR1 without stop codon.

Next, ligation reaction was set to insert GPR1 between the cut sites in multiple cloning sites of the vectors. After 3-hour ligation incubation at 16˚C, the products were directly transformed to competent *E.coli* cells. On the following day, three colonies from each plate were inoculated into liquid LB containing 100 µg/mL ampicillin, and the plasmids were isolated after 16-hour incubation. The plasmids were treated with *BamHI* and *EcoRI* enzymes in double digestion reactions for 2-hour and the sizes of DNA fragments were controlled on agarose gel (Figure 3.3).

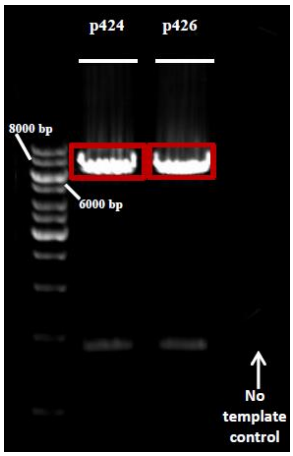

Figure 3.2 p24 and p426 vectors were digested with BamHI and EcoRI restriction enzymes. Lane 1: Gene Ruler 1 kb DNA Ladder. Lane 2: Digested p424 vector (~ 6500 bp). Lane 3: Digested p426 vector (~ 6700 bp). Lane 4: No template control

Figure 3.3 p424 and p426 vectors were digested with BamHI and EcoRI. Lane 1: Gene Ruler 1 kb DNA Ladder. Lane 2: No template control. Lane 3: GPR1 (~2,9 kb) in p424 (~6,5 kb). Lane 4: GPR1 (~2,9 kb) in p426 (~6,7 kb).

There is a final step for confirmation of the constructs, sequencing. Since the sequence of whole vector was not known, sequencing primers were designed only for GPR1 (Appendix B). After the sequences of these constructs were confirmed by sequencing results, we continued using them in further steps.

3.2. Construction of Gpr1p fusion proteins with fluorescent proteins

3.2.1. Tagging Gpr1p from 854th position with both full length and split fragments of fluorescent proteins using overlap extension PCR cloning method

The choice of insertion positions was not completely random. Insertion of FPs into 854th position of Gpr1 was experimentally decided after a previous study on tagging Ste2p from its C-terminus and C-tail, where seventh TM domain left the membrane, in our research lab.

For insertion of both full length and split fragments of EGFP (Accession number: AAB02574) and mCherry (Accession number: ACO48282) proteins into 854th position of Gpr1 using overlap extension PCR cloning method, two successive polymerase chain reactions were set. In the first step, the gene to be inserted in the second reaction is amplified with the flanking sequences of the insertion site at both ends. Then, in the second step, the product of first PCR is used as primer for the amplification of template DNA. Hence, considering the information, the primer pairs were designed having 15 complementary bases to the genes of fluorescent proteins and 30 complementary bases around 2562th bp position of GPR1 (Appendix B). In addition, the split positions of fluorescent proteins, EGFP between 158th -159th positions and mCherry between 159th-160th positions, were optimized previously by colleagues in our lab.

First, EGFP, mCherry, N-EGFP, C-EGFP, N-mCherry and C-mCherry cDNAs with Gpr1 flanking ends were amplified, and their sizes were confirmed by agarose gel electrophoresis (Figure 3.4). Next, DNA fragments in red boxes were extracted from agarose gel to be used as primers in the second PCR in which either p424 or p426 carrying GPR1 gene was template DNA. Since the amplified sequences in first step had homologous sequences with the intended insertion site in GPR1, they could act as primers. The optimized PCR mixture and conditions (see *Chapter 2*) for Phire II HS enzyme was applied. Then, these second PCR products were treated with *DpnI* to digest the plasmids that had methylated GATC sequences. Since methylated residues cannot be produced by polymerase chain reaction, they were required to be removed from the mix before next reaction. After *DpnI* treatment, the plasmids were transformed into competent *E.coli* cells. On the following days, same protocol was applied to amplify the plasmids. Purified plasmids were treated with *BamHI* and *EcoRI* enzymes in the double digestion reactions. In this step, we expected two distinct bands representing GPR1 carrying cDNA of fluorescent protein fragments and the vector in each lane (Figure 3.5).

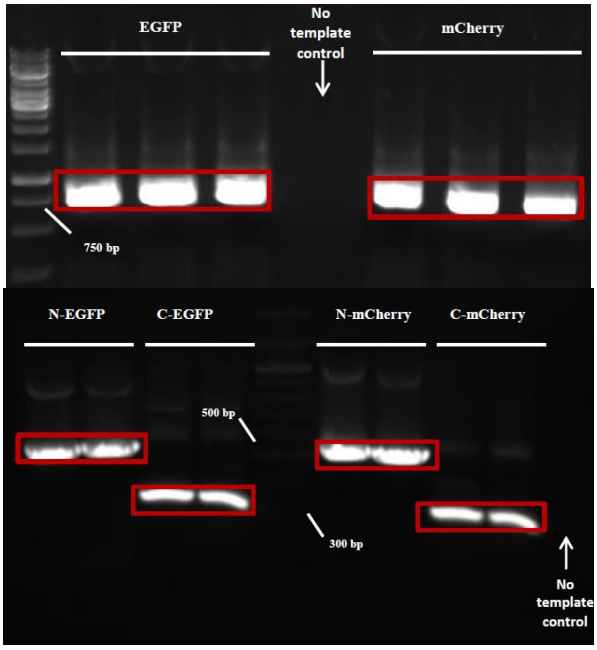

Figure 3.4 Fluorescent proteins were amplified with 30 bp flankings shown in red boxes. Gel image 1 (at the top)- Lane 1: Gene Ruler 1 kb DNA Ladder. Lane 2-4: EGFP (~750 bp). Lane 5: No template control. Lane 6-8: mCherry (~750 bp). Gel image 2 (at the bottom)- Lane 1-2: N-EGFP (~500 bp). Lane 3-4: C-EGFP (~300 bp). Lane 5: Gene Ruler 1 kb Plus DNA Ladder. Lane 6-7: N-mCherry (~500 bp). Lane 8-9: C-mCherry (~300 bp). Lane 10: No template control.

The size match alone does not give enough confirmation about the accuracy of the sequences, so they were sent for sequencing. Sequencing primers were designed according to information of GPR1 and cDNAs of fluorescent proteins (Appendix B). The results arrived from the company confirmed FP labeled GPR1 sequences. However, in the following steps, there were problems with expressions of these labeled proteins. The problem might result from mutations in the promoter region of expression vectors introduced during polymerase chain reactions. Eventually, the problem was fixed by transferring the GPR1+ tags into the empty vectors, which had not been subjected to any polymerase chain reactions, via cut sites they reside between.

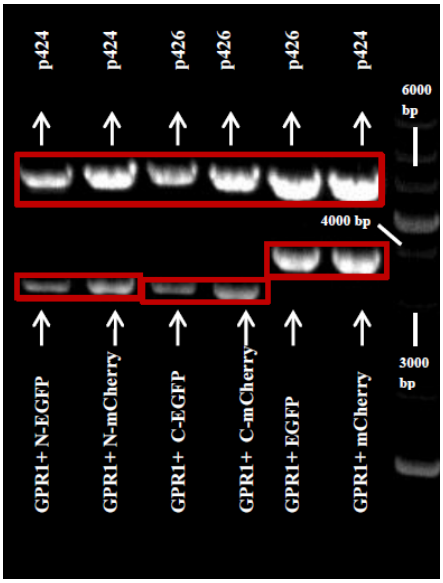

Figure 3.5 Constructed plasmids were digested with BamHI and EcoRI for confirmation of the sizes of DNA fragments shown in the boxes. Lane 1: GPR1+N-EGFP (~3,5 kb)_p424 (~6,5 kb). Lane 2: GPR1+N-mCherry (~3,5 kb) _p424 (~6,5 kb). Lane 3: GPR1+C-EGFP (~3,5 kb)_p426 (~6,5 kb). Lane 4: GPR1+C-mCherry (~3,5 kb)_p426 (~6,5 kb). Lane 5: GPR1+ EGFP (~3,7 kb)_p426 (~6,5 kb). Lane 6: GPR1+mCherry (~3,7 kb)_p424 (~6,5 kb). Lane 7: Gene Ruler 1 kb Plus DNA Ladder.

3.2.2. Tagging Gpr1p from C-terminus with both full length and split fragments of fluorescent proteins

For tagging Gpr1 receptor from its carboxy terminus, firstly, cDNAs of fluorescent proteins were cloned into yeast expression vectors. Since we had GPR1 that was ready-to-insert between *BamHI* and *EcoRI* in multiple cloning sites of the vectors, two other cut sites, *SalI and XhoI*, were chosen to insert coding sequences of fluorescent proteins. The main reason of this pair choice was their location. Because these sites are located at the end of multiple cloning sites that enables us to keep other cut sites in case of use later, and next to the site where GPR1 inserted that means fluorescent protein will be expressed at the end of protein, as planned at the beginning. Primer pairs were designed to insert *SalI*, GTCGAC, and XhoI, CTCGAG, sequences to 5' and 3' ends of the genes of fluorescent proteins, respectively (Appendix B). Using the optimized PCR conditions and mixtures for One Taq polymerase enzyme listed in *Chapter 2*, cDNAs cut sites added at the ends

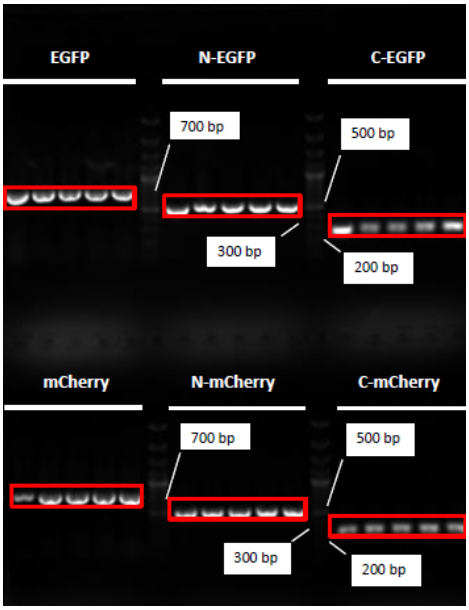

Figure 3.6 PCR products of fluorescent protein cDNAs with cut sites. Gel image 1 (at the top)- Lane1-5: EGFP (~700 bp). Lane 6: Gene Ruler 100 bp plus DNA Ladder. Lane 7-11: N-EGFP (~500 bp). Lane 12: Gene Ruler 100 bp plus DNA Ladder. Lane 13-17: C-EGFP (~300 bp). Gel image 2 (at the bottom) - Lane1-5: mCherry (~700 bp). Lane 6: Gene Ruler 100 bp plus DNA Ladder. Lane 7-11: N-mCherry (~500 bp). Lane 12: Gene Ruler 100 bp plus DNA Ladder. Lane 13-17: C-mCherry (~300 bp).

were amplified. The sizes of PCR products were confirmed by agarose gel electrophoresis (Figure 3.6).

DNA fragments shown in red boxes were excised and purified from agarose gel. Then, all these products, and p424 and p426 vectors were digested with *SalI* and *XhoI* restriction enzymes. Digested cDNAs were purified by PCR purification kit whereas digested vectors were run on and extracted from the gel. Ligation reaction was set to insert cDNAs into the digested p424 and p426 vectors. After 3-hour ligation incubation, the plasmids were transformed into competent *E.coli* cells. Next, plasmids were isolated from the cells grown in liquid media, and digested with *SalI* and *XhoI* enzymes to control the ligation. The products of double digestion reactions were run on 1% agarose gel and as expected there are two different DNA bands in each lane, one for FP and one for the vector (Figure 3.7).

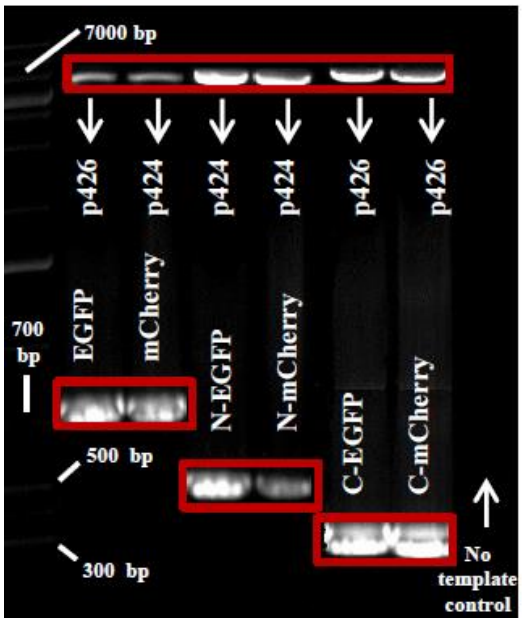

Figure 3.7 Constructed plasmids were digested with SalI and XhoI for confirmation of the sizes of DNA fragments. Lane1: Gene Ruler 1 kb Plus DNA Ladder. Lane 2: EGFP (~700 bp)_p426 (~6,5 kb). Lane 3: mCherry (~700 bp)_p424 (~6,5 kb). Lane 4: N-EGFP (~500 bp)_p424 (~6,5 kb). Lane 5: N-mCherry (~500 bp)_p424 (~6,5 kb). Lane 6: C-EGFP (~300 bp)_p426 (~6,5 kb). Lane 7: C-mCherry (~300 bp)_p426 (~6,5 kb). Lane 8: No template control.

After size confirmation, these constructs, and p424 and p426 vectors carrying GPR1 gene were digested with *BamHI* and *EcoRI* enzymes. At the end of 3-hour digestion incubation, these digested plasmids were run on 1% agarose gel to distinguish the digested fragments in each reaction tube. Next, plasmids carrying cDNAs of fluorescent proteins and GPR1 bands were identified and extracted from the gel for further ligation reaction. The ligation protocol and incubation time applied in earlier steps were repeated in this step as well. The ligation products were directly transformed into competent *E.coli* cells. Plasmids amplified by *E.coli* cells were then isolated, and digested with *BamHI* and *XhoI.* At this point, we expected to see two distinct bands representing GPR1+ full length or split cDNA fragments of fluorescent proteins, and the expression vectors, p424 or p426, in the lanes of agarose gel as shown in Figure 3.8. Finally, the sequences of those constructs were also confirmed by sequencing, and they were used in following experiments.

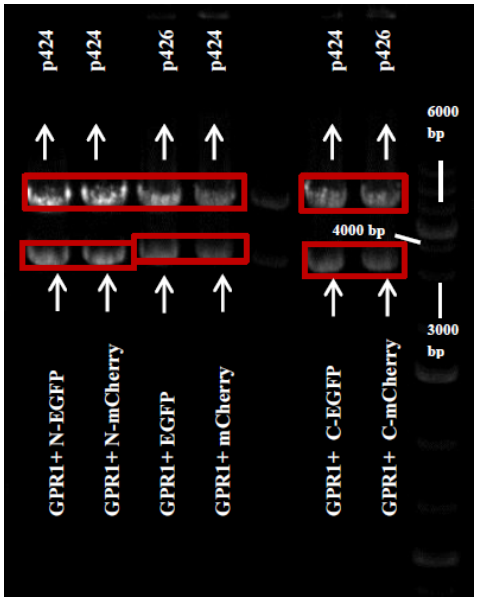

Figure 3.8 Constructed plasmids were digested with BamHI and XhoI for confirmation of the sizes of DNA fragments. Lane 1: GPR1+N-EGFP (~3,5 kb)_p424 (~6,5 kb). Lane 2: GPR1+N-mCherry (~3,5 kb) _p424 (~6,5 kb). Lane 3: GPR1+ EGFP (~3,7 kb)_p426 (~6,5 kb). Lane 4: GPR1+mCherry (~3,7 kb)_p424 (~6,5 kb). Lane 6: GPR1+C-EGFP (~3,5 kb)_p424 (~6,5 kb). Lane 7: GPR1+C-mCherry (~3,5 kb)_p426 (~6,5 kb). Lane 8: Gene Ruler 1 kb Plus DNA Ladder.

3.3. Construction of Ste2p fusion proteins with fluorescent proteins

Ste2 receptor was cloned into p424 and p426 expression vectors, tagged with full length fluorescent proteins at its 304th position by overlap extension PCR method as well. The constructs were separately transformed into a yeast strain named DK102 (*ste2::HIS3*). After confirmation of the plasmids by both imaging with confocal microscopy and growth arrest assay (Halo assay), yeast cells were transformed with plasmids carrying reciprocal labeled Ste2 proteins for FRET analysis (Kumas, 2012). All these work was carried out by a colleague in the lab. In our study, we used single transformant yeast cells for detection of Gpr1-Ste2 heterodimers and double transformant yeast cells as positive controls.

3.4. Functionality assessment of Gpr1 proteins in *Saccharomyces cerevisiae*

For detection and comparison of locations of Gpr1 homodimers in eukaryotic cells, two yeast strains were used in the study: W303-1A (wild type) and LK5 (*gpr1::LEU2*). The plasmids that were size- and sequence- confirmed, were

individually transformed into those yeast cells. The auxotrophy marker genes in expression vectors, *TRP*- in p424 and *URA*- in p426, enabled us to get expected transformants in corresponding minimal selective media. FP-tagged Gpr1 proteins in two groups of cells were expected to be as functional as in natural form. Hence, two different experiments were conducted to compare the functionality of receptors in wild type and mutant cells. First, growth curves of different groups were assessed by OD600 nm-based indirect measurements. Typical growth curve is composed of three distinct phases: lag, exponential (log) and stationary phase. We observed typical S-shape growth rate pattern in the different groups of cells which varied in the time required to reach stationary phase. The graph simply shows the difference in required time as 10-hour for wild type (W303-1A), and 12-hour for *gpr1Δ* (LK5) cells (Figure 3.9.a). This difference was an expected result since the cells that do not express functional Gpr1 receptors were reported to show delayed increased in volume size and growth (Xue *et al.*, 1998). Next, the growth rate of these cells was compared with the transformants received individual plasmids carrying Gpr1-EGFP, Gpr1-mCherry and Gpr1 without tag (Figure 3.9.b). From the graph, it is observed that delayed growth in *gpr1Δ* (LK5) cells was successfully recovered after transfection of genetically modified GPR1, and those cell groups showed growth rate pattern very similar to wild type cells.

Activation of cAMP pathway by glucose is known as a transient event which is immediately stimulated upon glucose sensing in the extracellular site by Gpr1p. Hence, we decided to check cAMP levels in different strains and compare them with wild-type. As a result of the experiment, stimulation of a rapid increase in the intracellular cAMP level upon the addition of glucose to yeast cells grown on a non-fermentable carbon source, for instance glycerol, was observed in wild type (W303-1A), GPR1 without tag *gpr1Δ*, GPR1-EGFP *gpr1Δ*, GPR1-mCherry *gpr1Δ* cells, but not *gpr1Δ* cells (Figure 3.10). Thus, we concluded that this cAMP response is not completely absent in *gpr1Δ* cells. However, it is delayed, and not as strong as in the case of other strains. In fact, this cAMP response is the result of slow, side mechanisms that transmit the signal of glucose sensing after a while compared to the GPCR system.

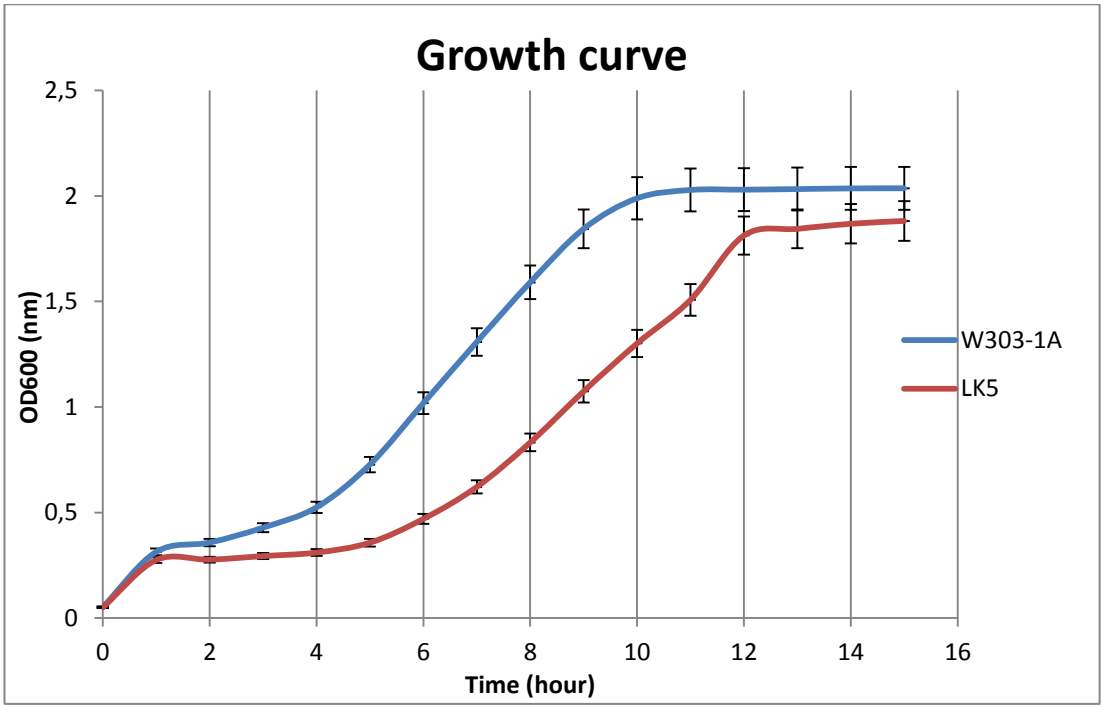

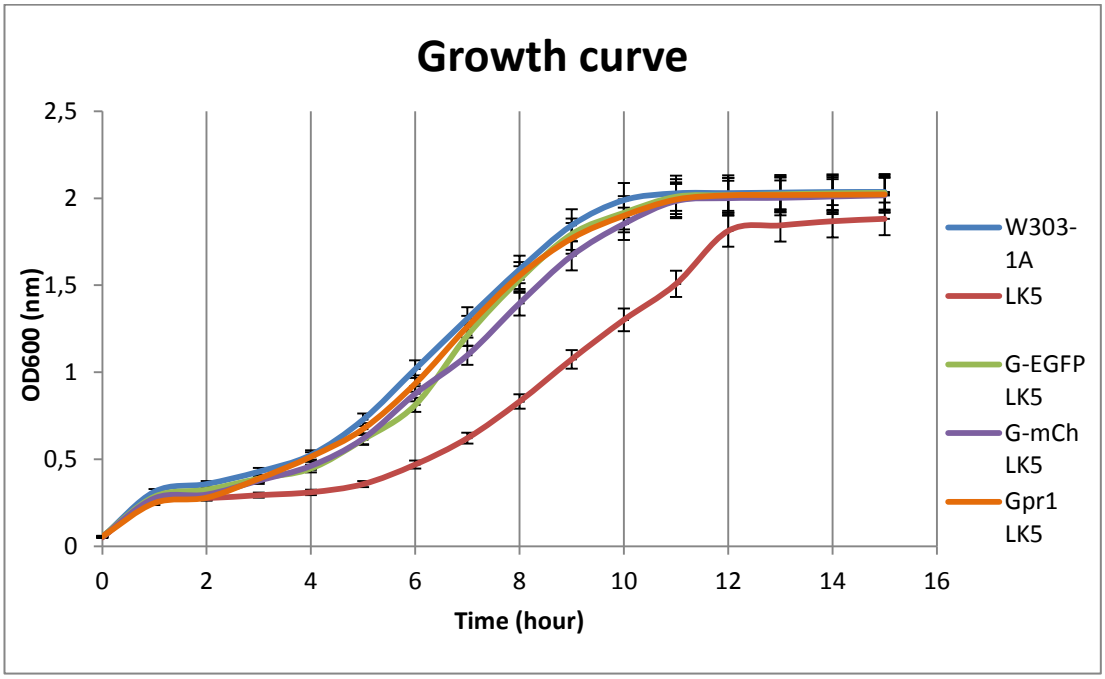

Figure 3.9 Growth Curves of Saccharomyces cerevisiae. a) Growth of wild type (W303-1A), *gpr1Δ* (LK5), and b) *gpr1Δ* (LK5) cells transformed with GPR1-EGFP, GPR1-mCherry and GPR1 without tag was monitored by recording OD values at 600 nm on an hourly basis for 16 hours.

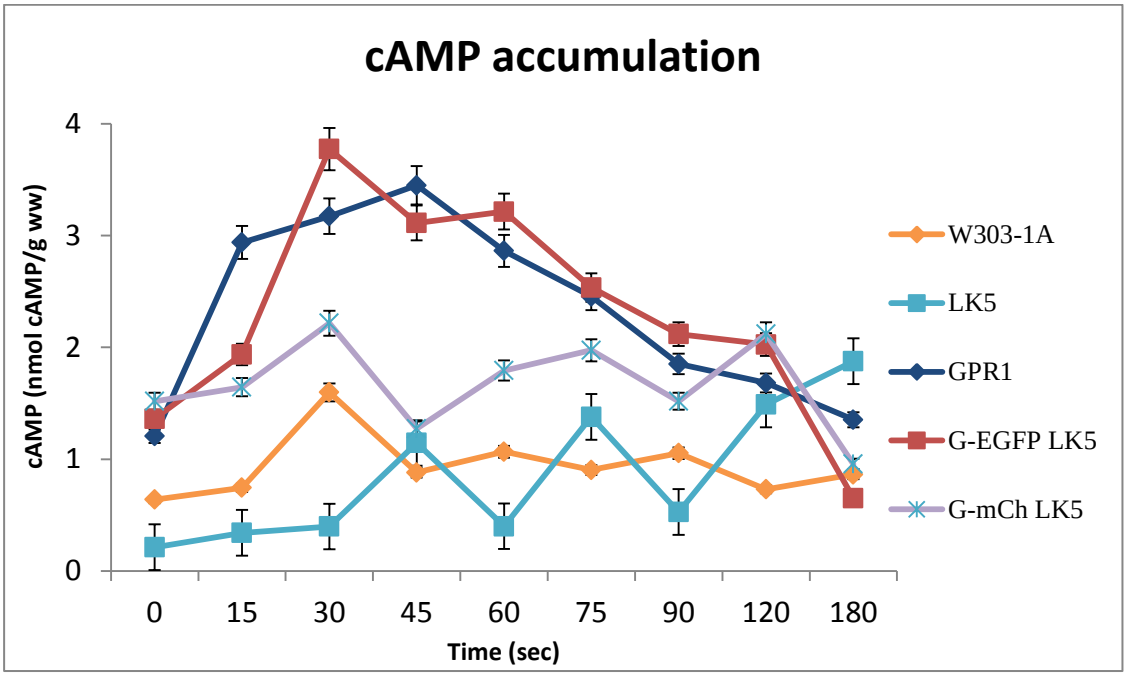

Figure 3.10 Stimulation of cAMP accumulation by glucose. Glucose (500 mM) was added to glycerol-grown cells of wild-type and GPR1 mutants. Strains: wild type (W303-1A), *gpr1Δ* (LK5), GPR1 without tag *gpr1Δ* , GPR1-EGFP *gpr1Δ* , GPR1-mCherry *gpr1Δ.* Error bars indicates standard deviation.

3.5. Detection of GPCR dimers in *Saccharomyces cerevisiae*

3.5.1. Detection of Gpr1 homodimers in *Saccharomyces cerevisiae*

At the end of single step transformation, 12 different cell populations were produced from wild type (W303-1A), *gpr1Δ* (LK5) strain (Table 3.1). Then, the groups were visualized under wide field fluorescence and laser scanning confocal microscope. During first imaging sessions, yeast cells were too mobile and it was impossible to take stable images to work on. Therefore, YPD, nutrient rich medium containing 0.4 % agar, was prepared to stabilize yeast cells for the following sessions. However, since this medium had dark-brown color due to high concentration of caramelized sugar, the background signal was too high that caused confusing effects in spectral bleedthrough calculations during FRET analysis. Finally, MLTU medium containing 0.4 % agar was chosen to be used during imaging of yeast cells due to its light color.

Table 3.1 12 different cell groups of both wild type (W303-1A), gpr1Δ (LK5) strains generated after transformation. 854th and C-terminus indicates the positions where FPs were inserted in GPR1 sequence.

Gpr1 854th position	**Gpr1 C-terminus**
Gpr1^{854}+EGFP	Gpr1+EGFP
Gpr1^{854}+mCherry	Gpr1+mCherry
Gpr1^{854}+N-EGFP	Gpr1+N-EGFP
Gpr1^{854}+C-EGFP	Gpr1+C-EGFP
Gpr1^{854}+N-mCherry	Gpr1+N-mCherry
Gpr1^{854}+C-mCherry	Gpr1+C-mCherry

The confocal microscope images of full length EGFP and mCherry labeled Gpr1 expressing cells of both strains were presented in Figure 3.11 and 3.12. Since split fragments were not functional alone, there was no signal from the cells transformed with those constructs, as expected.

However, we only observed signals from cells expressing Gpr1 tagged at 854th position, not the ones labeled from C-terminus. There are a few example studies in the literature previously tried to insert different tags at C-terminus or very close to this position of Gpr1 receptor. In fact, those trials were unsuccessful attempts, like our case. Moreover, scientists still have no consensus on the specific role and the location of this tail of the receptor. Generally, when the primary sequence of the receptor was submitted to different, widely used bioinformatics tools, the results were pooled in two groups: the tail was located at the extracellular region or in the cytoplasmic site. In either case, the results of our study supported the conclusion made by Xue and his colleagues (1998) as a result of a pioneer study, which suggested as the C-tail seemed to be significant for some step in the production or stabilization of Gpr1 (Xue *et.al.*,1998).

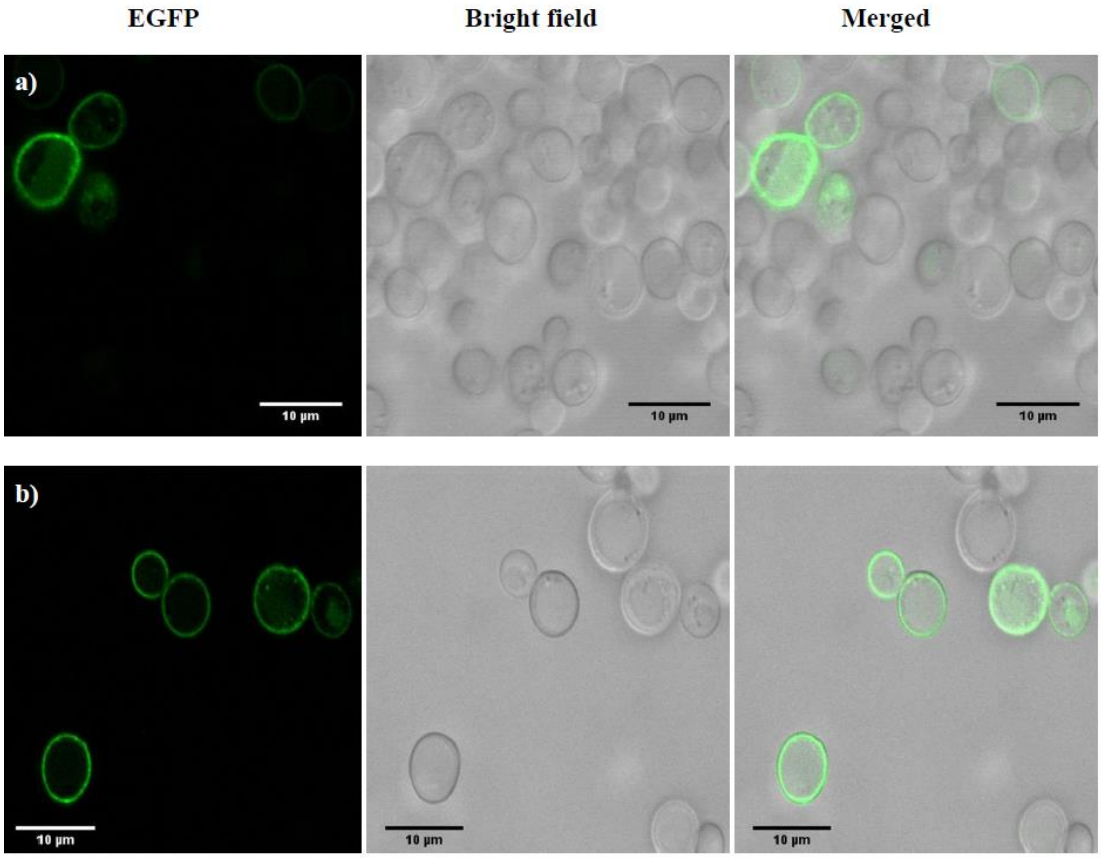

Figure 3.11 Full length EGFP labeled Gpr1 expressing a) wild type (W303-1A) and b) gpr1Δ (LK5) cells. Patterns of green signals in gpr1Δ mutant cells are very similar to wild type cells. These are only representative images for ten fields in a culture. The confocal images were taken by Zeiss LSM 510 Plan-Apochromat 63x/1.40 Oil DIC M27 objective. Scale bar: 10 µm.

After confirmation of labeled Gpr1 expression in both strains, these cells were transformed with the plasmids carrying reciprocal tagged Gpr1. For instance, yeast cells that transformed with p424 vectors containing EGFP tagged GPR1 in first step would receive p426 carrying mCherry tagged GPR1 sequence in second step of transformation. In this multiple-step transformation design, desired colonies were acquired with the help of different auxotrophy markers carried on the vectors. At the end of this step, 3 different yeast groups were generated for each strain. The double transformant cells were examined under wide field fluorescence and laser scanning confocal microscope, and the images were taken using previously adjusted settings for FRET analysis.

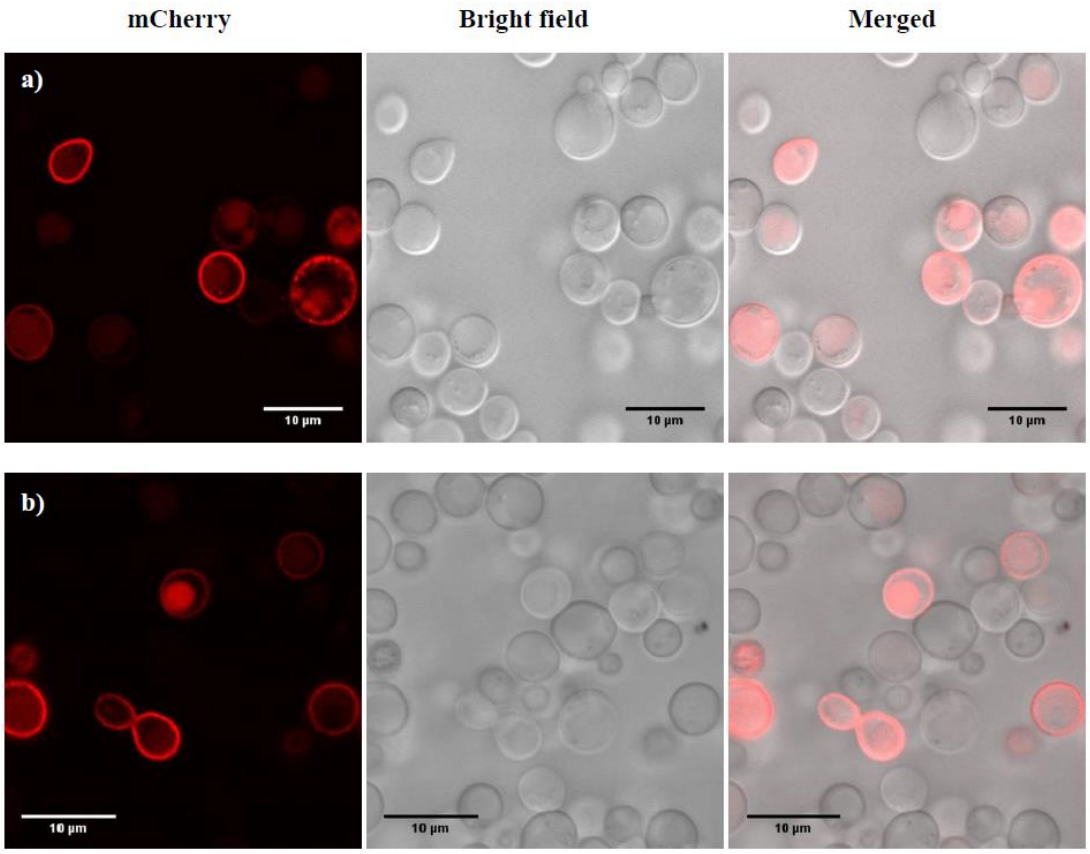

Figure 3.12 Full length mCherry labeled Gpr1 expressing a) wild type (W303-1A) and b) gpr1Δ (LK5) cells. Patterns of red signals in gpr1Δ mutant cells are very similar to wild type cells. These are only representative images for ten fields in a culture. The confocal images were taken by Zeiss LSM 510 Plan-Apochromat 63x/1.40 Oil DIC M27 objective. Scale bar: 10 µm.

For FRET analysis, besides images of double transformants, images of single transformant cells were acquired to calculate spectral bleed-through between green and red channels. Since the aim of this method was to detect the energy transfer between FPs, spectral bleed through calculation was a crucial step which enabled us to eliminate signal results from cross-talk between spectra of the FPs. For a single field in a culture, the images in four different channels were acquired; EGFP, FRET, mCherry and bright field. Afterwards, multi-colored images representing the cellular regions with different FRET efficiencies were prepared using PixFRET plugin of Image J program. Every single image was processed using PixFRET, and the data represented in histogram of FRET window of the program was recorded as in pixel

counts, mean of FRET efficiency and processed cell number (Figure 3.13). The range from 0-50 indicates FRET efficiency percentage, and data sets were generated for the following efficiency intervals from every individual image: 1-10%, 10-20%, 20-30%, 30-40% and 40-50%. Moreover, all data sets were used to calculate mean of FRET efficiency, pixel distribution over different FRET efficiency intervals and the distance between interacting fluorophores. Figure 3.14 and 3.15 shows representative FRET images of wild type (W303-1A) and *gpr1Δ* (LK5) cells, respectively.

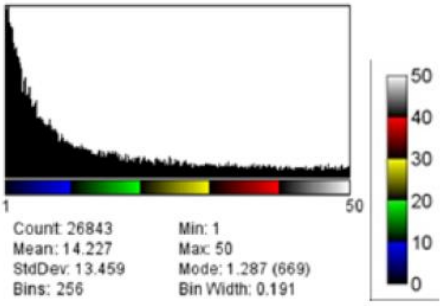

Figure 3.13 Representative image of FRET histogram in Image J-PixFRET. The histogram shows pixel distribution over different intervals of FRET efficiency.

The multi-colored FRET images showed us where Gpr1 homodimers were located in different yeast cells. Unlike the hypothesis set at the beginning, Gpr1 homodimers were detected not only on the plasma membrane but also in intracellular compartments of different strains as well. In a previous study in our research group showed that biogenesis and modifications of Gpr1 proteins occur within ER and Golgi, and the proteins are transported within COPII coated transport vesicles by co-localization experiments (Süder, 2013). Considering the results of this study and the information from literature, it can be concluded that Gpr1 homodimers may be transported through ER or Golgi within COPII vesicles to the plasma membrane and during their journey to the PM, they may form dimers in the transport vesicles. In addition to the results supporting anterograde traffic pathway, the internalization of Gpr1 proteins was shown using late endosome marker in a co-localization experiment. As a result, it was suggested that endocytic vesicles internalize the

proteins, then, maturate into late endosomes. Depending on these findings, FRET signal acquired from Gpr1 dimers in the cell may arise from late endosomes that return the membrane proteins to the appropriate compartment according to their sorting signals.

Further statistical analysis on data sets revealed the quantitative difference between FRET efficiencies of Gpr1 homodimers in different strains. The mean of FRET efficiency data of wild type (W303-1A) and *gpr1Δ* (LK5) strains were analyzed and compared using paired t-test in Graphpad Prism considering $p < 0.05$ statistically significant. As a result, it was understood that the FRET efficiency was significantly higher in transformants of mutant cells compared to wild type group ($p<0.05$) (Figure 3.16). This statistical difference might be a result of Gpr1 overexpression in wild type cells after transfection of FP-tagged Gpr1 proteins. Increase in the number of tagged and untagged Gpr1 in the cell might make it difficult for fluorophores to find each other and stand close enough to interact. Furthermore, since FRET method only allowed us to detect energy transfer between FP-pair, there was no way for detection of interactions between tagged and untagged Gpr1 receptors using this method. Pixel counts in FRET images were used to categorize cell groups in different FRET intervals (Figure 3.17). The summary of the analysis showed that in ~35 % of wild. type cells, 1-10% and in ~30 % of the population, 10-20% mean FRET efficiency was observed. In contrast, in the majority of the GPR1 mutants, 1-10% mean FRET efficiency was observed. In addition, 40-50% FRET, the highest efficiency, was observed in ~8 % of wild type cells whereas the result was only ~1 % in the mutant population. High percentage of cells with highest level of mean FRET efficiency might also be a result of overexpression in wild type cells. Although the number of receptors produced at a time increased, the total area occupied by receptors would be constant. This might cause localization of the tagged receptors even closer in the cell compared to *gpr1Δ* cells.

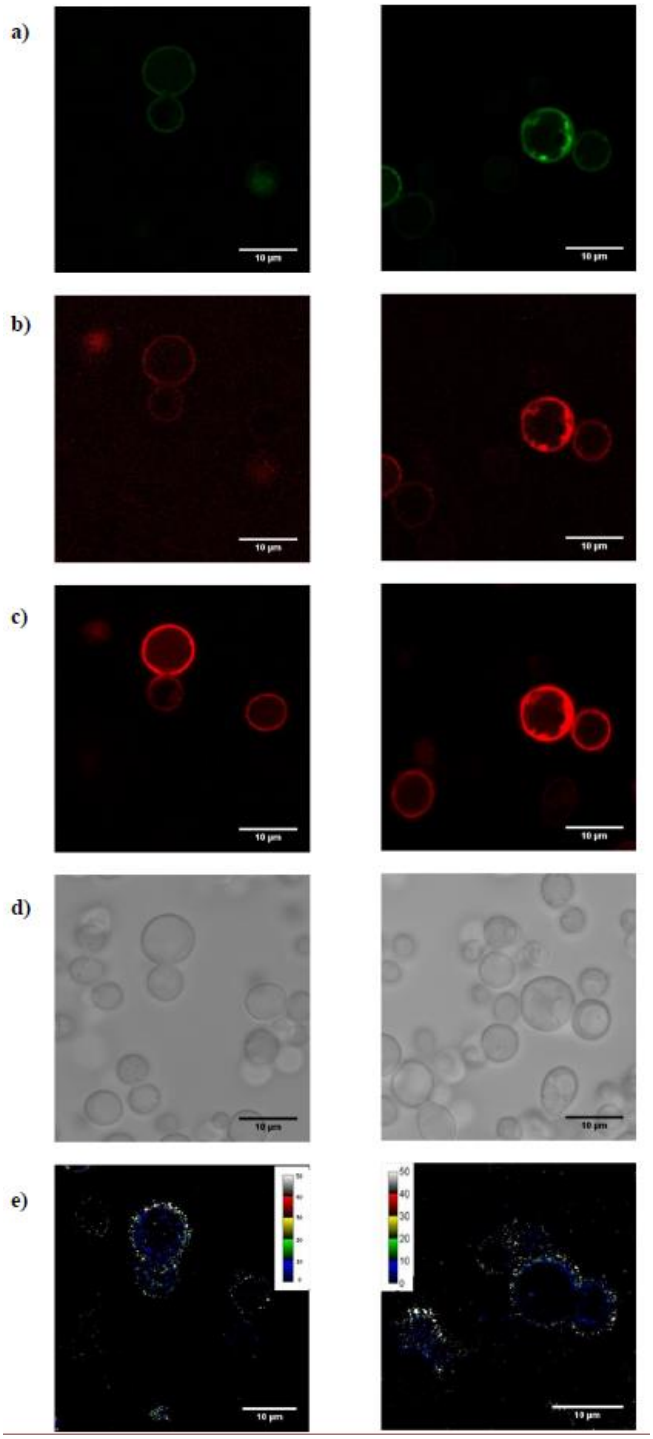

Figure 3.14 Representative FRET images of wild type (W303-1A) cells. The FRET image was processed using Image J-PixFRET. Calibration bar shows 1-50 % FRET efficiency. a) Images from EGFP channel, b) Images from FRET channel, c) Images from mCherry channel, d) Bright field image, e) FRET images. The confocal images were taken by Zeiss LSM 510 Plan-Apochromat 63x/1.40 Oil DIC M27 objective. Scale bar: 10 µm.

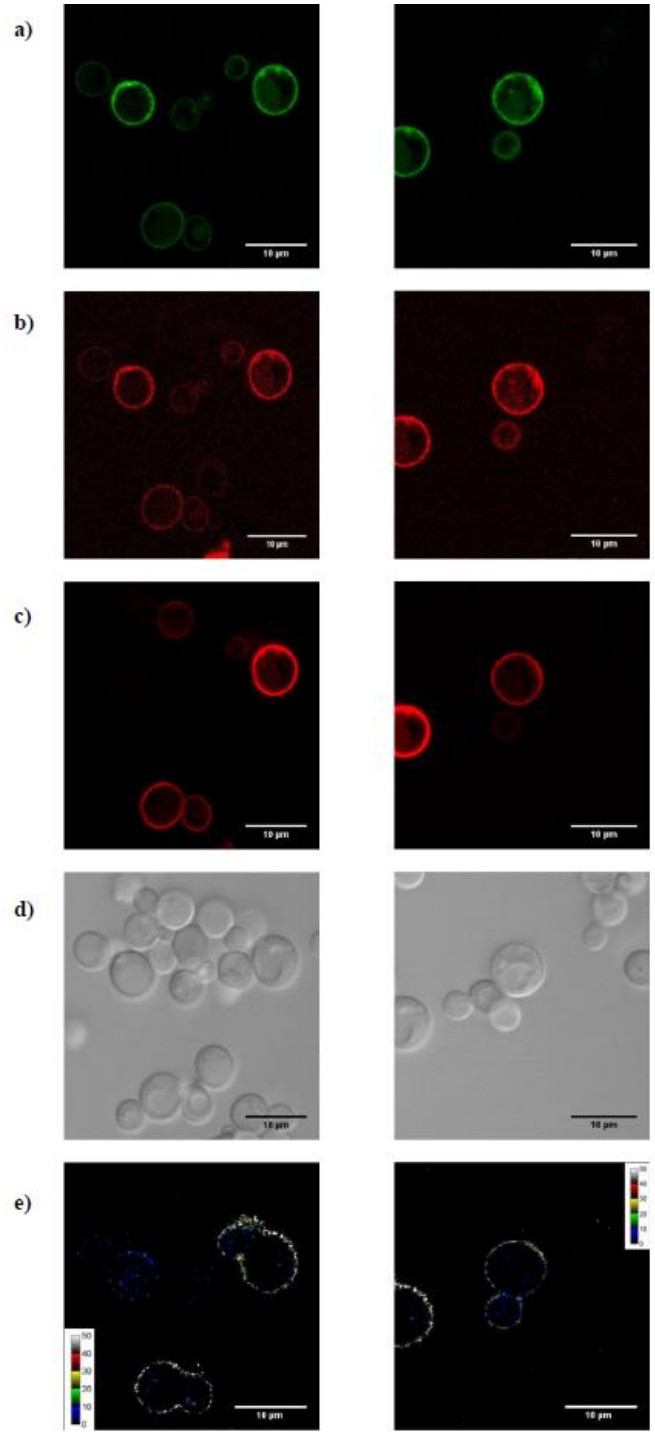

Figure 3.15 Representative FRET images of gpr1Δ (LK5) cells. The FRET image was processed using Image J-PixFRET. Calibration bar shows 1-50 % FRET efficiency. a) Images from EGFP channel, b) Images from FRET channel, c) Images from mCherry channel, d) Bright field image, e) FRET images. The confocal images were taken by Zeiss LSM 510 Plan-Apochromat 63x/1.40 Oil DIC M27 objective. Scale bar: 10 µm.

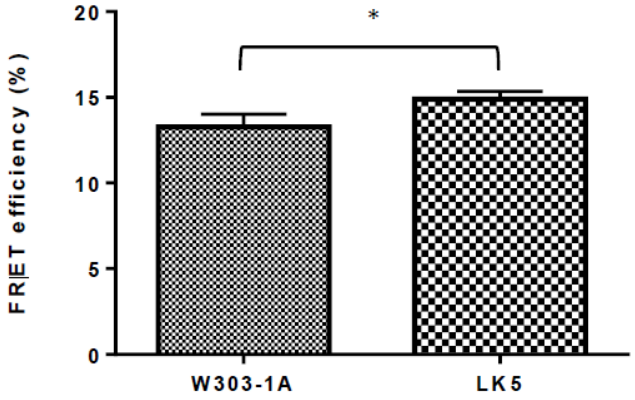

Figure 3.16 Comparison of FRET efficiency data of wild type (W303-1A) and gpr1Δ (LK5) cells. The mean of FRET efficiency was significantly high in LK5 cells *(p< 0.05). Error bars indicate standard error of the mean (SEM). Sample size for wild type cells is 196, and for gpr1Δ mutant cells 192.

The distance, *R*, between interacting fluorophores was calculated using the formula $E = \frac{1}{1+(\frac{R}{R0})^6}$ that R_0 is 51 A˚, a constant value for EGFP-mCherry pair. The basic principle in the equation is that the higher the efficiency, the lower the distance between fluorescent proteins. Therefore, the proteins were in their closest position where the FRET efficiency varies between 40-50%, and the distance was 52.90 A˚ in wild type, 52.65 A˚ in mutant cells. In fact, when the distribution of FRET values

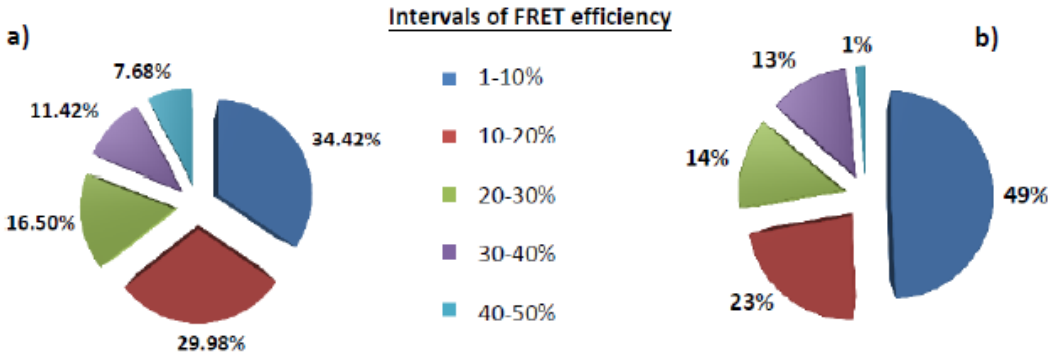

Figure 3.17 Distribution of different FRET intervals in the cell populations, a) wild type (W303-1A), b) gpr1Δ (LK5). Each piece of the chart represents a FRET interval listed in the center of the figure, and the data labels on the chart gives the percentage of the cells observed with indicated FRET level.

Table 3.2 Distance between fluorescent proteins in different FRET intervals. The distance is calculated using efficiency formula, *E*, for the mean value of each interval.

	W303-1A	LK5
FRET intervals	**R (Distance in A°)**	**R (Distance in A°)**
1-10%	82.06	83.35
10-20%	68.48	68.57
20-30%	61.50	61.39
30-40%	56.78	56.53
40-50%	52.90	52.65

over the cells were analyzed, it is observed that in both yeast populations, the highest value was on the cell membrane.

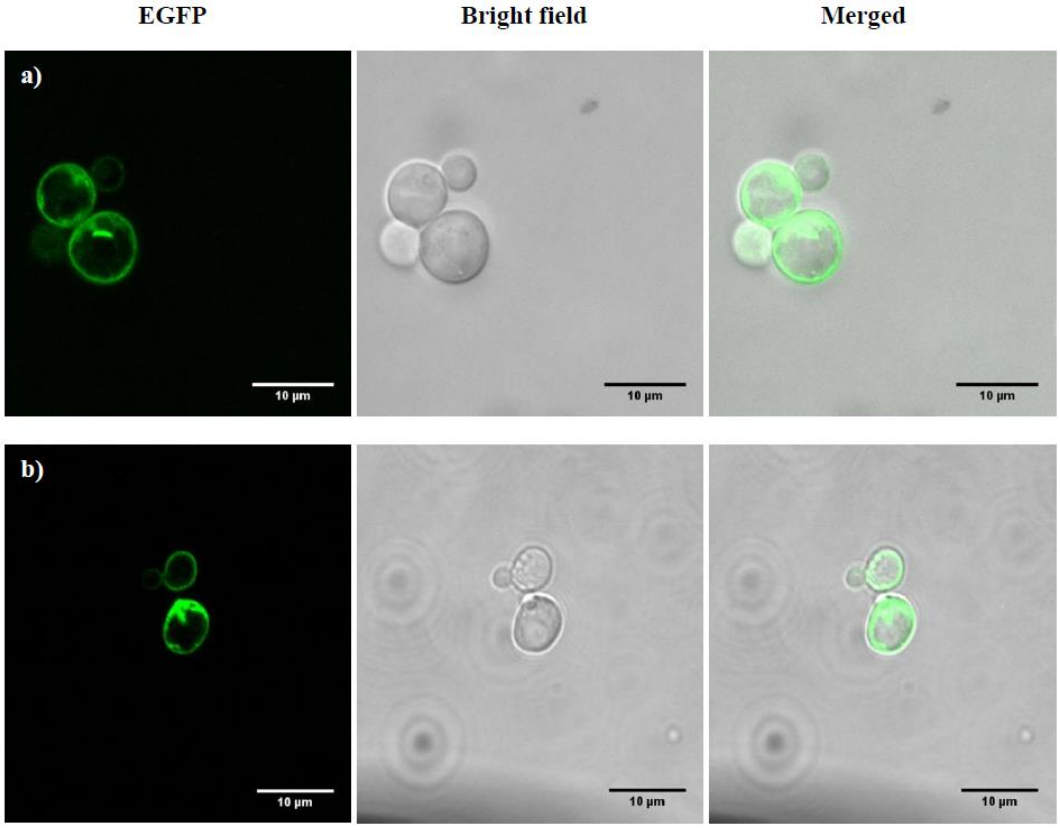

Figure 3.18 Split EGFP labeled Gpr1 expressing a) wild type (W303-1A) and b) gpr1Δ (LK5) cells. Patterns of green signals in gpr1Δ mutant cells are very similar to wild type. These are only representative images for ten fields in a culture. The confocal images were taken by Zeiss LSM 510 Plan-Apochromat 63x/1.40 Oil DIC M27 objective. Scale bar: 10 µm.

The outcome of split fluorescent protein complementation assay supported the results of FRET experiments as well. As we mentioned earlier, if two non-functional fragments come close enough to re-assemble like in formation of dimers, then, there would be a detectable green or red signal. After double transformation, the cells expected to have received both N- and C-split fragments of EGFP or mCherry were visualized under fluorescence and confocal microscope. The expected green and red signals were successfully observed inside the cell and on PM of both wild type and mutant cells (Figure 3.18 and 3.19). Thereby, it is concluded that together with FRET results, Gpr1 receptors form dimer structure probably during their biogenesis, activity on PM, anterograde and retrograde pathways.

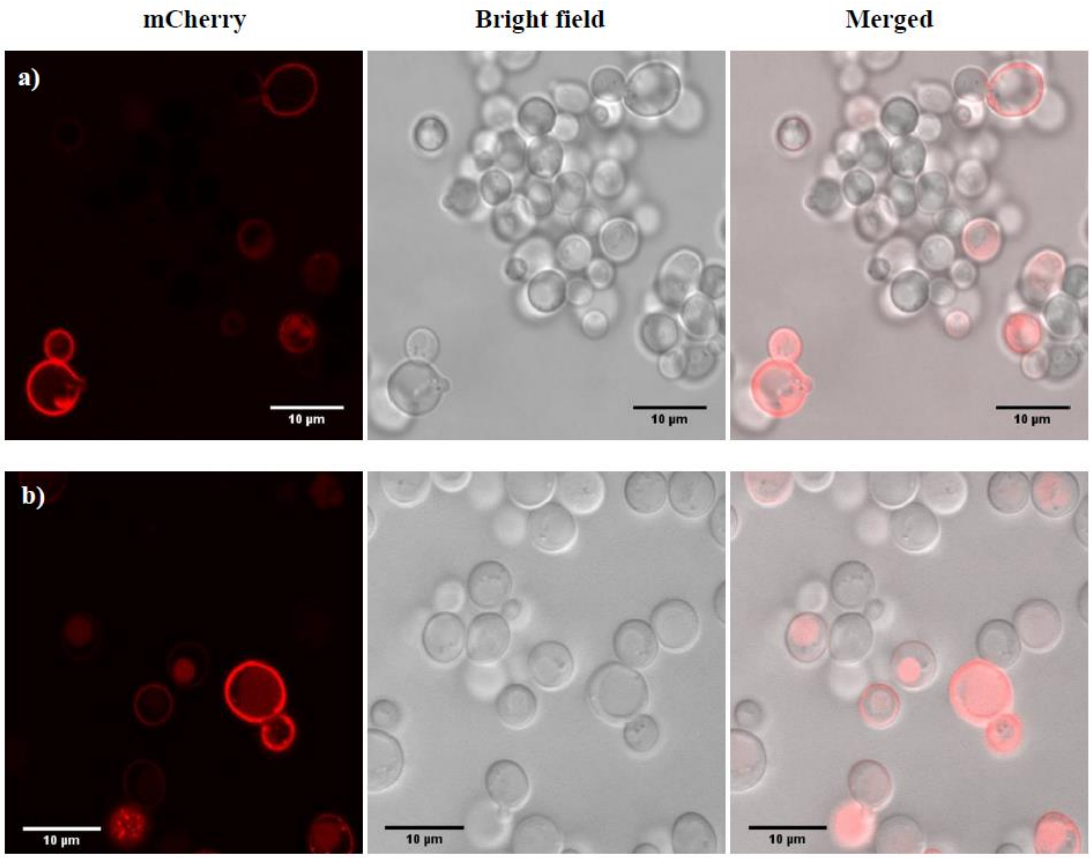

Figure 3.19 Split mCherry labeled Gpr1 expressing a) wild type (W303-1A) and b) gpr1Δ (LK5) cells. Patterns of red signals in gpr1Δ mutant cells are very similar to wild type. These are only representative images for ten fields in a culture. The confocal images were taken by Zeiss LSM 510 Plan-Apochromat 63x/1.40 Oil DIC M27 objective. Scale bar: 10 µm.

3.5.2. Detection of Gpr1-Ste2 heterodimers in *Saccharomyces cerevisiae*

Gpr1-Ste2 heterodimers were studied in other *Saccharomyces cerevisiae* strain, DK102. mCherry tagged Ste2 expressing strain was already engineered, thus, we transferred the plasmids containing EGFP tagged GPR1 into both empty DK102, and Ste2-mCherry expressing cells (Figure 3.20). Afterwards, the single transformants were used for spectral bleed-through calculations during FRET analysis of double transformants (Figure 3.21).

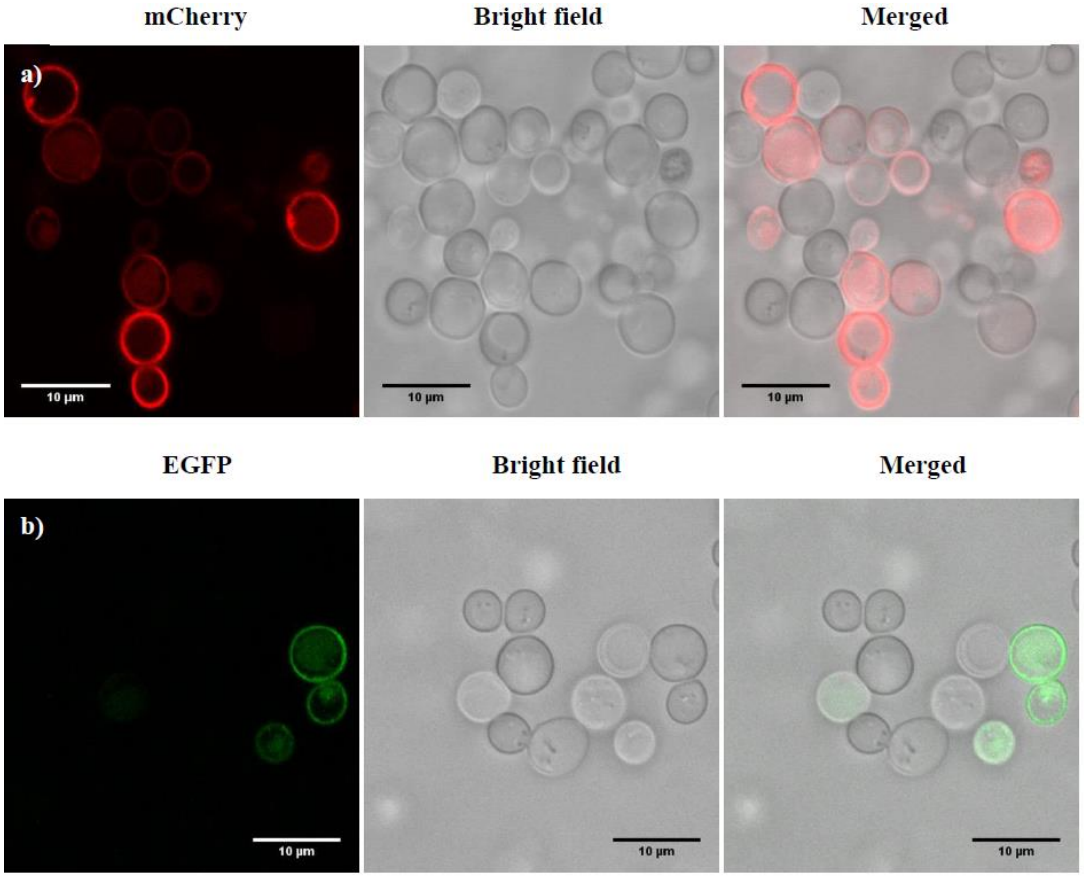

Figure 3.20 DK102 (ste2::HIS3) cells expressing a) mCherry tagged Ste2 receptors, and b) EGFP tagged Gpr1 receptors. The confocal image was taken by Zeiss LSM 510 Plan-Apochromat 63x/1.40 Oil DIC M27 objective. Scale bar: 10 µm.

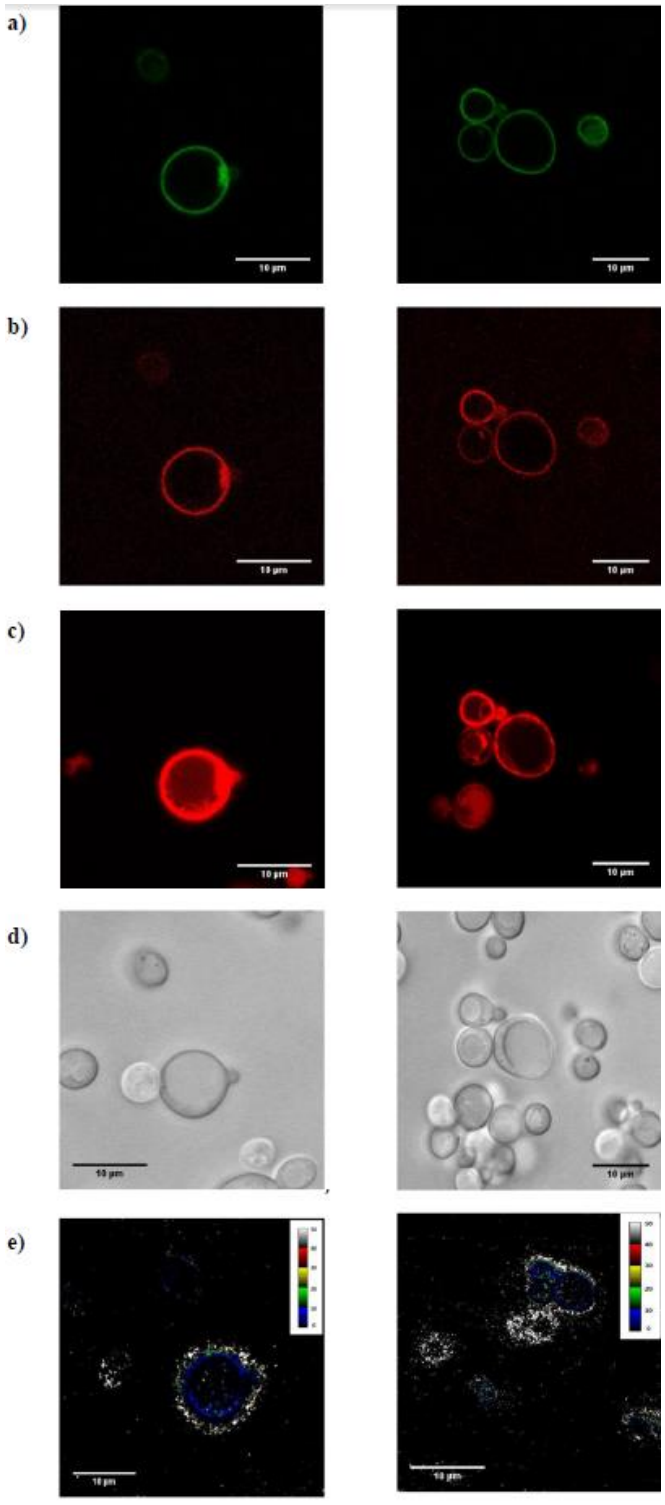

Figure 3.21 Representative FRET images of DK102 (ste2::HIS3) cells. The FRET image was processed using Image J-PixFRET. Calibration bar shows 1-50 % FRET efficiency. a) Images from EGFP channel, b) Images from FRET channel, c) Images from mCherry channel, d) Bright field image, e) FRET images. The confocal images were taken by Zeiss LSM 510 Plan-Apochromat 63x/1.40 Oil DIC M27 objective. Scale bar: 10 µm.

The analysis process was exactly same with Gpr1 homodimer case. The FRET images were processed and the data sets from histograms were collected for the efficiency, distance and cell distribution calculations. The mean of FRET efficiency in the case of Gpr1-Ste2 proteins was compared with the value of Ste2 homodimers in DK102 cells retrieved from a previous study in our lab. This data was also compared using paired t-test in Graphpad Prism considering $p < 0.05$ statistically significant. As a result, FRET level of Ste2 homodimers was significantly higher than the level of Gpr1-Ste2 heterodimers in DK102. For a fair comparison, the dimers must be studied in *gpr1Δ* (LK5) cells as well. Unfortunately, due to time limitation, this is listed as further study.

Distribution of different FRET values over cell population was analyzed using pixel counts and represented in Figure 3.22. 1-10% FRET was observed in approximately one third of the population and other FRET intervals were observed almost equally distributed over the population.

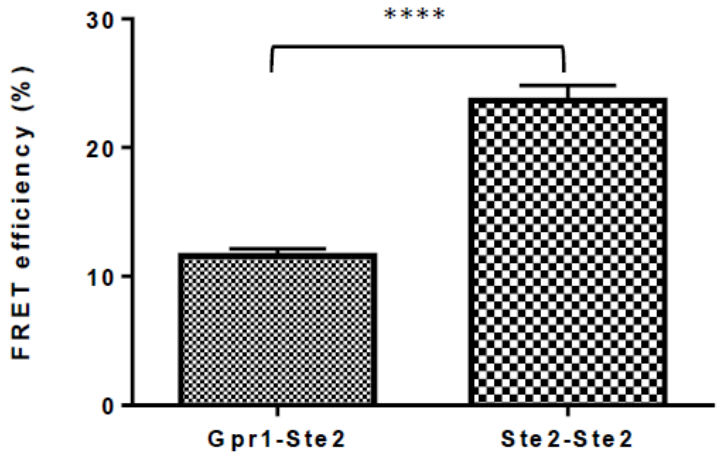

Figure 3.22 Comparison of FRET efficiency data of Gpr1-Ste2 and Ste2-Ste2 dimers in DK102. The mean of FRET efficiency was significantly high in the case of Ste2-Ste2 homodimers ($p < 0.05$). Error bars indicates standard error of the mean (SEM). Sample size for Gpr1-Ste2 case is 145, and for Ste2-Ste2 is 40.

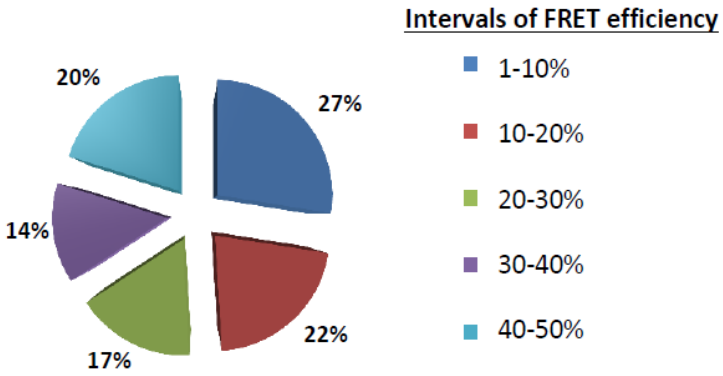

Figure 3.23 Distribution of different FRET intervals in DK102 population. Each piece of the chart represents a FRET interval from the list and the data labels on the chart gives the percentage of the cells observed with indicated FRET level.

Finally, the distance between interacting fluorophores was calculated using the mean of FRET efficiencies of individual intervals in the efficiency formula (Table 3.3). As it is inferred from the formula, the lowest FRET efficiency refers to the largest distance between the fluorophores. Therefore, the largest distance between the interacting proteins was 82.84 A˚ where FRET efficiency varies in between the lowest range, 1-10%, whereas the smallest distance was calculated as 52.84 A˚ in the range of high FRET efficiency, 40-50%.

Table 3.3 Distance between fluorescent proteins in different FRET intervals. The distance is calculated using efficiency formula, *E*, for the mean value of each interval.

	Gpr1-Ste2 in DK102
FRET intervals	**R(Distance in A˚)**
1-10%	82.84
10-20%	68.41
20-30%	58.71
30-40%	56.66
40-50%	52.84

CHAPTER 4

CONCLUSION

The hypothesis set at the beginning of the study was (i) revealing of Gpr1 homodimers on plasma membrane, where they show their main activity as surface receptors, and (ii) detection of Gpr1-Ste2 heterodimers also on plasma membrane using two powerful biophysical methods that allow imaging of protein-protein interactions in live yeast cells. At the end of the study, there are surprising additional results, besides expected ones:

- In this study, homodimerization of Gpr1 proteins in *Saccharomyces cerevisiae* was shown for the first time in the literature. These functional protein dimers were detected in both wild type and mutant cell groups suggesting that genetically engineered receptors could be successfully expressed and formed dimers in two different yeast strains.
- Gpr1 homodimers were detected on plasma membrane. In addition, they were observed in intracellular compartments, which resemble ER, Golgi or endocytic vesicles considering the previous studies. These findings suggest that Gpr1 proteins form homodimers during their biogenesis pathway, forward and reverse traffic between plasma membrane and cytosol as well as activity on plasma membrane.
- Like Gpr1 homodimers, Gpr1-Ste2 heterodimers were also observed on plasma membrane and over the cytosol by means of FRET and BiFC methods.

REFERENCES

Albertazzi, L., Arosio, D., Marchetti, L., Ricci, F., & Beltram, F. (2009). Quantitative FRET analysis with the EGFP-mCherry fluorescent protein pair. *Photochemistry and Photobiology*, *85*(1), 287–97. doi:10.1111/j.1751-1097.2008.00435.x

Angers, S., Salahpour, A., & Bouvier, M. (2002). Dimerization: an emerging concept for G protein-coupled receptor ontogeny and function. *Annual Review of Pharmacology and Toxicology*, *42*(1), 409–35. doi:10.1146/annurev.pharmtox.42.091701.082314

Antonny, B., D. Madden, S. Hamamoto, L. Orci, and R. Schekman, 2001 Dynamics of the COPII coat with GTP and stable analogues.Nat. Cell Biol. 3: 531–537.

Barkai, N., Rose, M. D., & Wingreen, N. S. (1998). Protease helps yeast find mating partners. *Nature*, *396*(6710), 422–3. doi:10.1038/24760

Barlowe, C. K., & Miller, E. a. (2013). Secretory protein biogenesis and traffic in the early secretory pathway. Genetics, 193(2), 383–410.

Barnard, E., McFerran, N. V., Trudgett, A., Nelson, J., & Timson, D. J. (2008). Detection and localisation of protein-protein interactions in Saccharomyces cerevisiae using a split-GFP method. *Fungal Genet Biol.*, *45*(5), 597–604. doi:10.1016/j.fgb.2008.01.003.

Bayburt, T. H. (2007). Transducin activation by nanoscale lipid bilayers containing one and two rhodopsins. *J Biol Chem*, *282*, 14875–14881.

Belinchón, M. M., & Gancedo, J. M. (2007a). Different signalling pathways mediate glucose induction of SUC2, HXT1 and pyruvate decarboxylase in yeast. *FEMS Yeast Research*, *7*(1), 40–7. doi:10.1111/j.1567-1364.2006.00136.x

Belinchón, M. M., & Gancedo, J. M. (2007b). Glucose controls multiple processes in Saccharomyces cerevisiae through diverse combinations of signaling pathways. *FEMS Yeast Research*, *7*(6), 808–18. doi:10.1111/j.1567-1364.2007.00236.x

Bert, T. E. H., & Bouvier, M. (1998). Structural and functional aspects of G protein-coupled receptor oligomerization. *Biochem Cell Biol*, *76*, 1–11.

Bonifacino, J., and B. Glick, 2004 The mechanisms of vesicle budding

and fusion. Cell 116: 153–166.

Bouvier, M. (2001). Oligomerization of G-protein-coupled transmitter receptors. *Nat Rev Neurosci*, *2*, 274–286.

Breitwieser, G. E. (2004). G protein-coupled receptor oligomerization: implications for G protein activation and cell signaling. *Circulation Research*, *94*(1), 17–27. doi:10.1161/01.RES.0000110420.68526.19

Brigance, W. T., C. Barlowe, and T. R. Graham, 2000 Organization of the yeast Golgi complex into at least four functionally distinct compartments. Mol. Biol. Cell 11: 171–182.

Brown, a J., Dyos, S. L., Whiteway, M. S., White, J. H., Watson, M. a, Marzioch, M., … Dowell, S. J. (2000). Functional coupling of mammalian receptors to the yeast mating pathway using novel yeast/mammalian G protein alpha-subunit chimeras. *Yeast (Chichester, England)*, *16*(1), 11–22. doi:10.1002/(SICI)1097-0061(20000115)16:1<11::AID-YEA502>3.0.CO;2-K

Budhwar, R., Lu, A., & Hirsch, J. P. (2010). Nutrient control of yeast PKA activity involves opposing effects on phosphorylation of the Bcy1 regulatory subunit. *Molecular Biology of the Cell*, *21*(21), 3749–58. doi:10.1091/mbc.E10-05-0388

Chen, X., C. VanValkenburgh, H. Liang, H. Fang, and N. Green,2001 Signal peptidase and oligosaccharyltransferase interact in a sequential and dependent manner within the endoplasmicreticulum. J. Biol. Chem. 276: 2411–2416.

Civelli, O., Reinscheid, R. K., Zhang, Y., Wang, Z., Fredriksson, R., & Schiöth, H. B. (2013). G protein-coupled receptor deorphanizations. *Annual Review of Pharmacology and Toxicology*, *53*, 127–46. doi:10.1146/annurev-pharmtox-010611-134548

Concepcion, F. (2002). The carboxyl-terminal domain is essential for rhodopsin transport in rod photoreceptors. *Vision Res*, *42*, 417–426.

Conrad, M., Schothorst, J., Kankipati, H. N., Van Zeebroeck, G., Rubio-Texeira, M., & Thevelein, J. M. (2014). Nutrient sensing and signaling in the yeast Saccharomyces cerevisiae. *FEMS Microbiology Reviews*, *38*(2), 254–99. doi:10.1111/1574-6976.12065

Croft, W., Hill, C., McCann, E., Bond, M., Esparza-Franco, M., Bennett, J., … Ladds, G. (2013). A physiologically required G protein-coupled receptor

(GPCR)-regulator of G protein signaling (RGS) interaction that compartmentalizes RGS activity. *The Journal of Biological Chemistry*, *288*(38), 27327–42. doi:10.1074/jbc.M113.497826

Daggett, K. a, & Sakmar, T. P. (2011). Site-specific *in vitro* and in vivo incorporation of molecular probes to study G-protein-coupled receptors. *Current Opinion in Chemical Biology*, *15*(3), 392–8. doi:10.1016/j.cbpa.2011.03.010

Dancourt, J., and C. Barlowe, 2010 Protein sorting receptors in the early secretory pathway. Annu. Rev. Biochem. 79: 777–802.

Defea, K. (2008). Beta-arrestins and heterotrimeric G-proteins: collaborators and competitors in signal transduction. *British Journal of Pharmacology*, *153*, 298–309. doi:10.1038/sj.bjp.0707508

d'Enfert, C., L. J. Wuestehube, T. Lila, and R. Schekman,1991 Sec12p-dependent membrane binding of the small GTP-binding protein Sar1p promotes formation of transport vesicles from the ER. J. Cell Biol. 114: 663–670.

Dohlman, H., & Thorner, J. (2001). Regulation of G protein-initiated signal transduction in yeast: paradigms and principles. *Annual Review of Biochemistry*, *70*, 703–54. Retrieved from http://www.annualreviews.org/doi/abs/10.1146/annurev.biochem.70.1.703

Dorer, R., Pryciak, P., & Hartwell, L. (1995). Saccharomyces cerevisiae cells execute a default pathway to select a mate in the absence of pheromone gradients. *The Journal of Cell Biology*, *131*(4), 845–861. Retrieved from http://jcb.rupress.org/content/131/4/845.abstract

Dorsam, R. T., & Gutkind, J. S. (2007). G-protein-coupled receptors and cancer. *Nature Reviews. Cancer*, *7*(2), 79–94. doi:10.1038/nrc2069

Elion, E. a. (2000). Pheromone response, mating and cell biology. *Current Opinion in Microbiology*, *3*(6), 573–81. Retrieved from http://www.ncbi.nlm.nih.gov/pubmed/11121776

Emr, S., B. S. Glick, A. D. Linstedt, J. Lippincott-Schwartz, A. Luini et al., 2009 Journeys through the Golgi–taking stock in a new era. J. Cell Biol. 187: 449–453.

Fan, J.-Y., Cui, Z.-Q., Wei, H.-P., Zhang, Z.-P., Zhou, Y.-F., Wang, Y.-P., & Zhang, X.-E. (2008). Split mCherry as a new red bimolecular fluorescence complementation system for visualizing protein-protein interactions in living cells. *Biochemical and Biophysical Research Communications*, *367*(1), 47–53. doi:10.1016/j.bbrc.2007.12.101

Ferré, S., Casadó, V., Devi, L. a, Filizola, M., Jockers, R., Lohse, M. J., … Guitart, X. (2014). G protein-coupled receptor oligomerization revisited: functional and pharmacological perspectives. *Pharmacological Reviews*, *66*(2), 413–34. doi:10.1124/pr.113.008052

Förster T. (1948). Intermolecular Energy Migration and Fluorescence. *Ann Phys*, *2*, 55–75.

Fredriksson, R., & Schiöth, H. B. (2005). The repertoire of G-protein-coupled receptors in fully sequenced genomes. *Molecular Pharmacology*, *67*(5), 1414–25. doi:10.1124/mol.104.009001

Gehret, A. U., Connelly, S. M., & Dumont, M. E. (2012). Functional and physical interactions among Saccharomyces cerevisiae α-factor receptors. *Eukaryotic Cell*, *11*(10), 1276–88. doi:10.1128/EC.00172-12

Giepmans, B. N., Adams, S. R., Ellisman, M. H., & Tsien, R. Y. (2006). No Title. *Science*, *312*, 217–224.

Gietz, D., St Jean, a, Woods, R. a, & Schiestl, R. H. (1992). Improved method for high efficiency transformation of intact yeast cells. *Nucleic Acids Research*, *20*(6), 1425. Retrieved from http://www.pubmedcentral.nih.gov/articlerender.fcgi?artid=312198&tool=pmcentrez&rendertype=abstract

González-Maeso, J. (2011). GPCR oligomers in pharmacology and signaling. *Molecular Brain*, *4*(1), 20. doi:10.1186/1756-6606-4-20

Graham, T. R., and S. D. Emr, 1991 Compartmental organization of Golgi-specific protein modification and vacuolar protein sorting events defined in a yeast sec18 (NSF) mutant. J. Cell Biol.114: 207–218.

Gurevich, V., & Gurevich, E. (2008). How and why do GPCRs dimerize? *Trends in Pharmacological Sciences*, *29*(5), 234–240. doi:10.1016/j.tips.2008.02.004.

Hann, B. C., C. J. Stirling, and P. Walter, 1992 SEC65 gene product is a subunit of

the yeast signal recognition particle required for its integrity. Nature 356: 532–533.

Harashima, T., & Heitman, J. (2002). The Galpha protein Gpa2 controls yeast differentiation by interacting with kelch repeat proteins that mimic Gbeta subunits. *Molecular Cell*, *10*(1), 163–73. Retrieved from http://www.ncbi.nlm.nih.gov/pubmed/12150916

Harashima, T., & Heitman, J. (2005). Galpha subunit Gpa2 recruits kelch repeat subunits that inhibit receptor-G protein coupling during cAMP-induced dimorphic transitions in Saccharomyces cerevisiae. *Molecular Biology of the Cell*, *16*(10), 4557–71. doi:10.1091/mbc.E05-05-0403

Hasan, M. T., Friedrich, R. W., Euler, T., Larkum, M. E., Giese, G., Both, M., … Denk, D. (2004). No Title. *PLoS Biol.*, *e163*.

Heldin, C. H. (1995). Dimerization of cell surface receptors in signal transduction. *Cell*, *80*(2), 213–23. Retrieved from http://www.ncbi.nlm.nih.gov/pubmed/7834741

Heng, B. C., Aubel, D., & Fussenegger, M. (2014). G protein-coupled receptors revisited: therapeutic applications inspired by synthetic biology. *Annual Review of Pharmacology and Toxicology*, *54*, 227–49. doi:10.1146/annurev-pharmtox-011613-135921

Jackson, C., & Hartwell, L. (1990). Courtship in S. cerevisiae: both cell types choose mating partners by responding to the strongest pheromone signal. *Cell*, *63*(5), 1039–51.

Kalab, P., & Pralle, A. (2008). No Title. *Methods in Enzymology*, *89*, 539–566.

Kalab, P., Pralle, A., Isacoff, E. Y., Heald, R., & Weis, K. (2006). No Title. *Nature*, *440*, 697–701.

Kaláb, P., & Soderholm, J. (2010). The design of Förster (fluorescence) resonance energy transfer (FRET)-based molecular sensors for Ran GTPase. *Methods (San Diego, Calif.)*, *51*(2), 220–32. doi:10.1016/j.ymeth.2010.01.022

Katritch, V., Cherezov, V., & Stevens, R. C. (2013). Structure-function of the G protein-coupled receptor superfamily. *Annual Review of Pharmacology and Toxicology*, *53*, 531–56. doi:10.1146/annurev-pharmtox-032112-135923

Kaupmann, K., Malitschek, B., Schuler, V., Heid, J., Froestl, W., Beck, P., … Shigemoto, R. (1998). GABABreceptor subtypes assemble into functional heteromeric complexes. *Nature*, *396*, 683–687.

Kim, H., Lee, B., Naider, F., & Becker, J. (2009). Identification of Specific Transmembrane Residues and Ligand-Induced Interface Changes Involved In Homo-Dimer Formation of A Yeast G Protein-Coupled Receptor. *Biochemistry*, *48*(46), 10976–10987. doi:10.1021/bi901291c.

Kim, K.-M., Lee, Y.-H., Akal-Strader, A., Uddin, M. S., Hauser, M., Naider, F., & Becker, J. M. (2012). Multiple regulatory roles of the carboxy terminus of Ste2p a yeast GPCR. *Pharmacological Research : The Official Journal of the Italian Pharmacological Society*, *65*(1), 31–40. doi:10.1016/j.phrs.2011.11.002

Kobilka, B. (2013). The Structural Basis of G-Protein-Coupled Receptor Signaling (Nobel Lecture). *Angewandte Chemie International Edition*, *52*(25), 6380–6388. doi:10.1002/anie.201302116.

Koelle, M. R. (2006). Heterotrimeric G protein signaling: Getting inside the cell. *Cell*, *126*(1), 25–7. doi:10.1016/j.cell.2006.06.026

Kraakman, L., Lemaire, K., Ma, P., Teunissen, a W., Donaton, M. C., Van Dijck, P., … Thevelein, J. M. (1999). A Saccharomyces cerevisiae G-protein coupled receptor, Gpr1, is specifically required for glucose activation of the cAMP pathway during the transition to growth on glucose. *Molecular Microbiology*, *32*(5), 1002–12. Retrieved from http://www.ncbi.nlm.nih.gov/pubmed/10361302

Kremers, G.-J., Gilbert, S. G., Cranfill, P. J., Davidson, M. W., & Piston, D. W. (2011). Fluorescent proteins at a glance. *Journal of Cell Science*, *124*(15), 2676–2676. doi:10.1242/jcs.095059

Kubler, E., Mosch, H.-U., Rupp, S., & Lisanti, M. P. (1997). Gpa2p, a G-protein -Subunit, Regulates Growth and Pseudohyphal Development in Saccharomyces cerevisiae via a cAMP-dependent Mechanism. *Journal of Biological Chemistry*, *272*(33), 20321–20323. doi:10.1074/jbc.272.33.20321

Kumaş, G. (2012). *Detecting G-Protein Coupled Receptor Interactions Using Enhanced Green Fluorescent Protein Reassembly*. Middle East Technical University.

Kuszak, A. J., Pitchiaya, S., Anand, J. P., Mosberg, H. I., Walter, N. G., & Sunahara, R. K. (2009). Purification and functional reconstitution of monomeric mu-opioid receptors: allosteric modulation of agonist binding by Gi2. *J Biol Chem*.

Lakowicz, J. R. (2006). Principles of Fluorescence Spectroscopy. *Springer Science*.

Leeuw, T., Wu, C., Schrag, J. D., Whiteway, M., Thomas, D. Y., & Leberer, E. (1998). Interaction of a G-protein beta-subunit with a conserved sequence in Ste20/PAK family protein kinases. *Nature*, *391*(6663), 191–5. doi:10.1038/34448

Lemaire, K., Van de Velde, S., Van Dijck, P., & Thevelein, J. M. (2004). Glucose and sucrose act as agonist and mannose as antagonist ligands of the G protein-coupled receptor Gpr1 in the yeast Saccharomyces cerevisiae. *Molecular Cell*, *16*(2), 293–9. doi:10.1016/j.molcel.2004.10.004

Li, J. (2004). Structure of bovine rhodopsin in a trigonal crystal form. *J Mol Biol*, *343*, 1409–1438.

Lohse, M. J. (2010). Dimerization in GPCR mobility and signaling. *Current Opinion in Pharmacology*, *10*(1), 53–8. doi:10.1016/j.coph.2009.10.007

Lorenz, M. C., Pan, X., Harashima, T., Cardenas, M. E., Xue, Y., Hirsch, J. P., & Heitman, J. (2000). The G protein-coupled receptor gpr1 is a nutrient sensor that regulates pseudohyphal differentiation in Saccharomyces cerevisiae. *Genetics*, *154*(2), 609–22. Retrieved from http://www.pubmedcentral.nih.gov/articlerender.fcgi?artid=1460933&tool=pmcentrez&rendertype=abstract

Lu, A., & Hirsch, J. (2005). Cyclic AMP-independent regulation of protein kinase A substrate phosphorylation by Kelch repeat proteins. *Eukaryotic Cell*, *4*(11). doi:10.1128/EC.4.11.1794

Madden, K., & Snyder, M. (1992). Specification of sites for polarized growth in Saccharomyces cerevisiae and the influence of external factors on site selection. *Molecular Biology of the Cell*, *3*(9), 1025–35. Retrieved from http://www.pubmedcentral.nih.gov/articlerender.fcgi?artid=275663&tool=pmcentrez&rendertype=abstract

Maeda, S., & Schertler, G. F. X. (2013). Production of GPCR and GPCR complexes for structure determination. *Current Opinion in Structural Biology*, *23*(3), 381–92. doi:10.1016/j.sbi.2013.04.006

Marinissen MJ, & Gutkind JS. (2001). *Trends Pharmacol Sci*, *22*(7), 368–76. Retrieved from http://www.ncbi.nlm.nih.gov/pubmed/11431032

Matsuoka, K., R. Schekman, L. Orci, and J. E. Heuser, 2001 Surface structure of the COPII-coated vesicle. Proc. Natl.Acad. Sci. USA 98: 13705–13709.

Maurel, D., Comps-Agrar, L., Brock, C., Rives, M. L., Bourrier, E., Ayoub, M. A., … Zeau, L. P. (2008). Cellsurface protein–protein interaction analysis with timeresolved FRET and snap-tag technologies: application to GPCR oligomerization. *Nat Methods*, *5*, 561–567.

Meng, J., Beverly, E., Marcelo, B., Mather, W., Nayak, S., Hasty, J., … Elston, T. C. (2011). No Title. *Science Signalling*, *4*(186), ra54. doi:10.1126/scisignal.2001763

Merlini, L., Dudin, O., & Martin, S. (2013). Mate and fuse: how yeast cells do it. *Open Biology*, *3*. Retrieved from http://dx.doi.org/10.1098/rsob.130008

Meyer, H. A., and E. Hartmann, 1997 The yeast SPC22/23 homolog Spc3p is essential for signal peptidase activity. J. Biol. Chem. 272: 13159–13164.

Milligan, G. (2009). G protein-coupled receptor hetero-dimerization: contribution to pharmacology and function. *British Journal of Pharmacology*, *158*(1), 5–14. doi:10.1111/j.1476-5381.2009.00169.x

Milligan, G., Ramsay, D., Pascal, G., & Carrillo, J. J. (2003). GPCR dimerisation. *Life Sciences*, *74*(2-3), 181–188. doi:10.1016/j.lfs.2003.09.005

Mossessova, E., L. C. Bickford, and J. Goldberg, 2003 SNARE selectivity of the COPII coat. Cell 114: 483–495.

Nakafuku, M., Obara, T., Kaibuchi, K., Miyajima, I., Miyajima, a, Itoh, H., … Kaziro, Y. (1988). Isolation of a second yeast Saccharomyces cerevisiae gene (GPA2) coding for guanine nucleotide-binding regulatory protein: studies on its structure and possible functions. *Proceedings of the National Academy of Sciences of the United States of America*, *85*(5), 1374–8. Retrieved from http://www.pubmedcentral.nih.gov/articlerender.fcgi?artid=279773&tool=pmcentrez&rendertype=abstract

Nakamura, Y., Ishii, J., & Kondo, A. (2013). Rapid, Facile Detection of Heterodimer Partners for Target Human G-Protein-Coupled Receptors Using a Modified Split-Ubiquitin Membrane Yeast Two-Hybrid System. *PloS One*, *8*(6), e66793. doi:10.1371/journal.pone.0066793

Nakano, A., D. Brada, and R. Schekman, 1988 A membrane glycoprotein,Sec12p, required for protein transport from the endoplasmic reticulum to the Golgi apparatus in yeast. J. Cell Biol.107: 851–863.

Nazarko, V. Y., Thevelein, J. M., & Sibirny, A. a. (2008). G-protein-coupled receptor Gpr1 and G-protein Gpa2 of cAMP-dependent signaling pathway are involved in glucose-induced pexophagy in the yeast Saccharomyces cerevisiae. *Cell Biology International*, *32*(5), 502–4. doi:10.1016/j.cellbi.2007.11.001

Nichols, A. S., Floyd, D. H., Bruinsma, S. P., Narzinski, K., & Baranski, T. J. (2013). Frizzled receptors signal through G proteins. *Cellular Signalling*, *25*(6), 1468–75. doi:10.1016/j.cellsig.2013.03.009

Nobles, M., Benians, A., & Tinker, A. (2005). Heterotrimeric G proteins precouple with G protein-coupled receptors in living cells. *Proceedings of the National Academy of Sciences of the United States of America*, *102*(51), 18706–11. doi:10.1073/pnas.0504778102

Nuoffer, C., A. Horvath, and H. Riezman, 1993 Analysis of the sequence requirements for glycosylphosphatidylinositol anchoring of Saccharomyces cerevisiae Gas1 protein. J. Biol. Chem.268: 10558–10563.

Ogg, S. C., W. P. Barz, and P. Walter, 1998 A functional GTPase domain, but not its transmembrane domain, is required for function of the SRP receptor beta-subunit. J. Cell Biol. 142:341–354.

Overton, M., Chinault, S., & Blumer, K. (2005). Oligomerization of G-protein-coupled receptors: lessons from the yeast Saccharomyces cerevisiae. *Eukaryotic Cell*, *4*(12), 1963–1970. doi:10.1128/EC.4.12.

Palczewski, K. (2000). Crystal structure of rhodopsin: A G protein-coupled receptor. *Science*, *289*, 739–745.

Palczewski, K. (2010). Oligomeric forms of G protein-coupled receptors (GPCRs). *Trends in Biochemical Sciences*, *35*(11), 595–600. doi:10.1016/j.tibs.2010.05.002.

Park, J. H., Scheerer, P., Hofmann, K. P., Choe, H.-W., & Ernst, O. P. (2008). Crystal structure of the ligand-free G-protein-coupled receptor opsin. *Nature*, *454*(7201), 183–7. doi:10.1038/nature07063

Peeters, K., & Thevelein, J. M. (2014). *Molecular Mechanisms in Yeast Carbon Metabolism*. (J. Piškur & C. Compagno, Eds.) (pp. 21–57). Berlin, Heidelberg: Springer Berlin Heidelberg. doi:10.1007/978-3-642-55013-3

Peeters, T., Versele, M., & Thevelein, J. M. (2007). Directly from Galpha to protein kinase A: the kelch repeat protein bypass of adenylate cyclase. *Trends in Biochemical Sciences*, *32*(12), 547–54. doi:10.1016/j.tibs.2007.09.011

Pincus, D., Ryan, C. J., Smith, R. D., Brent, R., & Resnekov, O. (2013). Assigning quantitative function to post-translational modifications reveals multiple sites of phosphorylation that tune yeast pheromone signaling output. *PloS One*, *8*(3), e56544. doi:10.1371/journal.pone.0056544

Piston, D. W., & Kremers, G. J. (2007). No Title. *Trends Biochem Sci*, *32*, 407–414.

Pittet, M., and A. Conzelmann, 2007 Biosynthesis and function of GPI proteins in the yeast Saccharomyces cerevisiae. Biochim.Biophys. Acta 1771: 405–420.

Potetinova, Z., Tantry, S., & Cohen, L. (2012). Large multiple transmembrane domain fragments of a G protein-coupled receptor: Biosynthesis, purification, and biophysical studies. *Bioploymers*, *98*(5), 485–500. doi:10.1002/bip.22122

Preininger, A. M., Meiler, J., & Hamm, H. E. (2013). Conformational flexibility and structural dynamics in GPCR-mediated G protein activation: a perspective. *Journal of Molecular Biology*, *425*(13), 2288–98. doi:10.1016/j.jmb.2013.04.011

Price, L., Strnad, J., Pausch, M., & Hadcock, J. (1996). Pharmacological characterization of the rat A2a adenosine receptor functionally coupled to the yeast pheromone response pathway. *Molecular Pharmacology*. Retrieved from http://molpharm.aspetjournals.org/content/50/4/829.short

Prinster, S. C. (2006). Alpha2C-adrenergic receptors exhibit enhanced surface expression and signaling upon association with beta2-adrenergic receptors. *J Pharmacol Exp Ther*, *318*, 974–981.

QIAGEN. (n.d.). Mating-Pheromone Response Pathway in Budding Yeast. Retrieved August 28, 2014, from http://www.qiagen.com/products/genes and pathways/pathway details.aspx?pwid=283

Rasmussen, S. G. (2007). Crystal structure of the human beta(2) adrenergic G-protein-coupled receptor. *Nature*, *450*, 383–387.

Richards, F. M. (1958). On the enzymic activity of subtilisin-modified ribonuclease. . *Proc Nat Acad Sci USA*, *44*, 162–166.

Rios, C. D., Jordan, B. a, Gomes, I., & Devi, L. a. (2001). G-protein-coupled receptor dimerization: modulation of receptor function. *Pharmacology & Therapeutics*, *92*(2-3), 71–87. Retrieved from http://www.ncbi.nlm.nih.gov/pubmed/11916530

RM, E., & T, R. (2009). New insights into GPCR function: implications for HTS. *Methods Mol Biol.*, *552*, 1–13. doi:10.1007/978-1-60327-317-6_1.

Rolland, F., De Winde, J. H., Lemaire, K., Boles, E., Thevelein, J. M., & Winderickx, J. (2000). Glucose-induced cAMP signalling in yeast requires both a G-protein coupled receptor system for extracellular glucose detection and a separable hexose kinase-dependent sensing process. *Molecular Microbiology*, *38*(2), 348–58. Retrieved from http://www.ncbi.nlm.nih.gov/pubmed/11069660

Rolland, F., Winderickx, J., & Thevelein, J. M. (2001). Glucose-sensing mechanisms in eukaryotic cells. *Trends in Biochemical Sciences*, *26*(5), 310–7. Retrieved from http://www.ncbi.nlm.nih.gov/pubmed/11343924

Rolland, F., Winderickx, J., & Thevelein, J. M. (2002). Glucose-sensing and -signalling mechanisms in yeast. *FEMS Yeast Research*, *2*(2), 183–201. Retrieved from http://www.ncbi.nlm.nih.gov/pubmed/12702307

Roy, R., Hohng, S., & Ha, T. (2008). No Title. *Nat Methods*, *5*, 507–516.

Rubio-Texeira, M., Van Zeebroeck, G., Voordeckers, K., & Thevelein, J. M. (2010). Saccharomyces cerevisiae plasma membrane nutrient sensors and their role in PKA signaling. *FEMS Yeast Research*, *10*(2), 134–49. doi:10.1111/j.1567-1364.2009.00587.x

Sahoo, H., Roccatano, D., Zacharias, M., Nau, W. M., & Soc, J. A. C. (2006). No Title. *128*, 8118–8119.

Santangelo, G. (2006). Glucose signaling in Saccharomyces cerevisiae. *Microbiology and Molecular Biology Reviews*, *70*(1), 253–282. doi:10.1128/MMBR.70.1.

Scheerer, P., Park, J. H., Hildebrand, P. W., Kim, Y. J., Krauss, N., Choe, H. W., … Ernst, O. P. (2008). Crystal structure of opsin in its Gprotein- interacting conformation. *Nature*, *455*, 497–502.

Schiöth, H. B., & Fredriksson, R. (2005). The GRAFS classification system of G-protein coupled receptors in comparative perspective. *General and Comparative Endocrinology*, *142*(1-2), 94–101. doi:10.1016/j.ygcen.2004.12.018

Schwarz, F., and M. Aebi, 2011 Mechanisms and principles of N-linked protein glycosylation. Curr. Opin. Struct. Biol. 21: 576–582.

Shaner, N. C., Lin, M. Z., McKeown, M. R., Steinbach, P. A., Hazelwood, K. L., Davidson, M. W., & Tsien, R. Y. (2008). No Title. *Nat. Methods*, *5*, 545–551.

Shaner, N., Steinbach, P., & Tsien, R. (2005). A guide to choosing fluorescent proteins. *Nature Methods*, *2*(12), 905–909. doi:10.1038/NMETH819

Shekhawat, S., & Ghosh, I. (2011). Split-protein systems: beyond binary protein–protein interactions. *Current Opinion in Chemical Biology*, *15*(6), 789–797. doi:10.1016/j.cbpa.2011.10.014.

Shikano, S., and M. Li, 2003 Membrane receptor trafficking:evidence of proximal and distal zones conferred by two independent endoplasmic reticulum localization signals. Proc.Natl. Acad. Sci. USA 100: 5783–5788.

Shyu, Y. J., Suarez, C. D., & Hu, C.-D. (2008). Visualization of ternary complexes in living cells by using a BiFC-based FRET assay. *Nature Protocols*, *3*(11), 1693–702. doi:10.1038/nprot.2008.157

Stefan, C. J., Overton M. C., & Blumer K. J. (1998). Mechanisms governing the activation and trafficking of yeast G protein-coupled receptors. *Molecular biology of the cell*, 9, 885-899.

Stirling, C. J., and E. W. Hewitt, 1992 The S. cerevisiae SEC65 gene encodes a component of yeast signal recognition particle with homology to human SRP19. Nature 356: 534–537.

Strahl-Bolsinger, S., M. Gentzsch, and W. Tanner, 1999 Protein Omannosylation. Biochim. Biophys. Acta 1426: 297–307.

Süder, I (2013). Labelingand optimization of organelle markers for co-localization

with yeast GPCR dimers. Middle East Technical University.

Surma, M. a, Klose, C., & Simons, K. (2012). Lipid-dependent protein sorting at the trans-Golgi network. Biochimica et biophysica acta, 1821(8), 1059–67.

Szidonya, L., Cserzo, M., & Hunyady, L. (2008). Dimerization and oligomerization of G-protein-coupled receptors: debated structures with established and emerging functions. *The Journal of Endocrinology*, *196*(3), 435–53. doi:10.1677/JOE-07-0573

Takanishi, C. L., Bykova, E. a, Cheng, W., & Zheng, J. (2006). GFP-based FRET analysis in live cells. *Brain Research*, *1091*(1), 132–9. doi:10.1016/j.brainres.2006.01.119

Tamaki, H. (2007). Glucose-stimulated cAMP-protein kinase A pathway in yeast Saccharomyces cerevisiae. *Journal of Bioscience and Bioengineering*, *104*(4), 245–50. doi:10.1263/jbb.104.245

Tamaki, H., Yun, C.-W., Mizutani, T., Tsuzuki, T., Takagi, Y., Shinozaki, M., … Kumagai, H. (2005). Glucose-dependent cell size is regulated by a G protein-coupled receptor system in yeast Saccharomyces cerevisiae. *Genes to Cells : Devoted to Molecular & Cellular Mechanisms*, *10*(3), 193–206. doi:10.1111/j.1365-2443.2005.00828.x

Terrillon, S., & Bouvier, M. (2004). No Title. *EMBO J*, *23*, 3950–3961.

Terrillon, S., & Bouvier, M. (2004). Roles of G-protein-coupled receptor dimerization. *EMBO Reports*, *5*(1), 30–4. doi:10.1038/sj.embor.7400052

Thevelein, J., Cauwenberg, L., Colombo, S., De Winde JH, Donation, M., Dumortier, F., … Winderickx, J. (2000). Nutrient-induced signal transduction through the protein kinase A pathway and its role in the control of metabolism, stress resistance, and growth in yeast. *Enzyme and Microbial Technology*, *26*(9-10), 819–825. Retrieved from http://www.ncbi.nlm.nih.gov/pubmed/10862891

Thevelein, J. M., Geladé, R., Holsbeeks, I., Lagatie, O., Popova, Y., Rolland, F., … Yan, B. (2005). Nutrient sensing systems for rapid activation of the protein kinase A pathway in yeast. *Biochemical Society Transactions*, *33*(Pt 1), 253–6. doi:10.1042/BST0330253

Thomas, B. J., & Rothstein, R. (1989). Elevated recombination rates in transcriptionally active DNA. *Cell*, *56*(4), 619–630. doi:10.1016/0092-8674(89)90584-9

Tsien, R. Y., & Med, K. J. (2006). No Title, *55*, 127–140.

Ullmann, A., Jacob, F., & Monod, J. (1967). Characterization by *in vitro* complementation of a peptide corresponding to an operator-proximal segment of beta-galactosidase structural gene of Escherichia coli. *J. Mol. Bio.*, *24*(2), 339–343.

Umanah, G. K. E., Huang, L.-Y., Maccarone, J. M., Naider, F., & Becker, J. M. (2011). Changes in conformation at the cytoplasmic ends of the fifth and sixth transmembrane helices of a yeast G protein-coupled receptor in response to ligand binding. *Biochemistry*, *50*(32), 6841–54. doi:10.1021/bi200254h

Van de Velde, S., & Thevelein, J. M. (2008). Cyclic AMP-protein kinase A and Snf1 signaling mechanisms underlie the superior potency of sucrose for induction of filamentation in Saccharomyces cerevisiae. *Eukaryotic Cell*, *7*(2), 286–93. doi:10.1128/EC.00276-07

Venkatakrishnan, a J., Deupi, X., Lebon, G., Tate, C. G., Schertler, G. F., & Babu, M. M. (2013). Molecular signatures of G-protein-coupled receptors. *Nature*, *494*(7436), 185–94. doi:10.1038/nature11896

Versele, M., de Winde, J. H., & Thevelein, J. M. (1999). A novel regulator of G protein signalling in yeast, Rgs2, downregulates glucose-activation of the cAMP pathway through direct inhibition of Gpa2. *The EMBO Journal*, *18*(20), 5577–91. doi:10.1093/emboj/18.20.5577

Versele, M., Lemaire, K., & Thevelein, J. M. (2001). Sex and sugar in yeast: two distinct GPCR systems. *EMBO Reports*, *2*(7), 574–9. doi:10.1093/embo-reports/kve132

Vidi, P.-A., Ejendal, K. F. K., Przybyla, J. a, & Watts, V. J. (2011). Fluorescent protein complementation assays: new tools to study G protein-coupled receptor oligomerization and GPCR-mediated signaling. *Molecular and Cellular Endocrinology*, *331*(2), 185–93. doi:10.1016/j.mce.2010.07.011

Vilardaga, J.-P., Agnati, L. F., Fuxe, K., & Ciruela, F. (2010). G-protein-coupled receptor heteromer dynamics. *Journal of Cell Science*, *123*(Pt 24), 4215–20. doi:10.1242/jcs.063354

Wang, Y., Chen, W., Simpson, D. M., & Elion, E. a. (2005). Cdc24 regulates nuclear shuttling and recruitment of the Ste5 scaffold to a heterotrimeric G protein in Saccharomyces cerevisiae. *The Journal of Biological Chemistry*, *280*(13), 13084–96. doi:10.1074/jbc.M410461200

Wettschureck, N., & Offermanns, S. (2005). Mammalian G proteins and their cell type specific functions. *Physiological Reviews*, *85*(4), 1159–204. doi:10.1152/physrev.00003.2005

White, J. F. (2007). Dimerization of the class A G protein-couple d neurotensin receptor NTS1 alters G protein interaction. *Proc Natl Acad Sci USA*, *104*, 12199–12204.

Whiteway, M., Wu, C., Leeuw, T., Clark, K., Fourest-Lieuvin, A., Thomas, D., & Leberer, E. (1995). Association of the yeast pheromone response G protein beta gamma subunits with the MAP kinase scaffold Ste5p. *Science*, *269*(5230), 1572–1575. doi:10.1126/science.7667635

Whorton, M. R., Bokoch, M. P., Rasmussen, S. G., Rasmussen, B., Zare, R. N., Kobilka, B., & Sunahara, R. K. (2007). A monomeric G protein-coupled receptor isolated in a high-density lipoprotein particle efficiently activates its G protein. *Proc Natl Acad Sci USA*, *104*, 7682–7687.

Whorton, M. R., Jastrzebska, B., Park, P. S., Fotiadis, D., Engel, A., Palczewski, K., & Sunahara, R. K. (2008). Efficient coupling of transducin to monomeric rhodopsin in a phospholipid bilayer. . *J Biol Chem*, *283*, 4387–4394.

Willhite, D. G., Brigati, J. R., Selcer, K. E., Denny, J. E., Duck, Z. a, & Wright, S. E. (2014). Pheromone responsiveness is regulated by components of the Gpr1p-mediated glucose sensing pathway in Saccharomyces cerevisiae. *Yeast (Chichester, England)*. doi:10.1002/yea.3030

Xue, C., Hsueh, Y., & Heitman, J. (2008). Magnificent seven: roles of G protein-coupled receptors in extracellular sensing in fungi. *FEMS Microbiology Reviews*, *32*(6), 1010–1032. doi:10.1111/j.1574-6976.2008.00131.x.

Xue, Y., Batlle, M., & Hirsch, J. P. (1998). GPR1 encodes a putative G protein-coupled receptor that associates with the Gpa2p Galpha subunit and functions in a Ras-independent pathway. *The EMBO Journal*, *17*(7), 1996–2007. doi:10.1093/emboj/17.7.1996

Yasuda, R., Harvey, C. D., Zhong, H., Sobczyk, A., Aelst, L. van, & Svoboda, K. (2006). No Title. *Nat Neurosci*, *9*, 283–291.

Zabrocki, P., Bastiaens, I., Delay, C., Bammens, T., Ghillebert, R., Pellens, K., … Winderickx, J. (2008). Phosphorylation, lipid raft interaction and traffic of alpha-synuclein in a yeast model for Parkinson. Biochimica et biophysica acta, 1783(10), 1767–80.

Zhu, X., & Wess, J. (1998). Truncated V2 vasopressin receptors as negative regulators of wild-type V2 receptor function. *Biochemistry*, *37*, 15773–15784.

Zimmermann, T., Rietdorf, J., Girod, A., Georget, V., & Pepperkok, R. (2002). Spectral imaging and linear un-mixing enables improved FRET efficiency with a novel GFP2-YFP pair. *FEBS Letters*, *531*, 245–49.

APPENDIX A

CODING SEQUENCES OF FUSION PROTEINS

A. EGFP cDNA Accession Number: AAB02574

```
ATGGTGAGCAAGGGCGAGGAGCTGTTCACCGGGGTGGTGCCCATCCTGGTCGAGCTG
GACGGCGACGTAAACGGCCACAAGTTCAGCGTGTCCGGCGAGGGCGAGGGCGATGCC
ACCTACGGCAAGCTGACCCTGAAGTTCATCTGCACCACCGGCAAGCTGCCCGTGCCC
TGGCCCACCCTCGTGACCACCCTGACCTACGGCGTGCAGTGCTTCAGCCGCTACCCC
GACCACATGAAGCAGCACGACTTCTTCAAGTCCGCCATGCCCGAAGGCTACGTCCAG
GAGCGCACCATCTTCTTCAAGGACGACGGCAACTACAAGACCCGCGCCGAGGTGAAG
TTCGAGGGCGACACCCTGGTGAACCGCATCGAGCTGAAGGGCATCGACTTCAAGGAG
GACGGCAACATCCTGGGGCACAAGCTGGAGTACAACTACAACAGCCACAACGTCTAT
ATCATGGCCGACAAGCAGAAGAACGGCATCAAGGTGAACTTCAAGATCCGCCACAAC
ATCGAGGACGGCAGCGTGCAGCTCGCCGACCACTACCAGCAGAACACCCCCATCGGC
GACGGCCCCGTGCTGCTGCCCGACAACCACTACCTGAGCACCCAGTCCAAGCTTAGC
AAAGACCCCAACGAGAAGCGCGATCACATGGTCCTGCTGGAGTTCGTGACCGCCGCC
GGGATCACTCTCGGCATGGACGAGCTGTACAAGTAA
```

B. mCherry cDNA Accession Number: ACO48282

```
ATGGTGAGCAAGGGCGAGGAGGATAACATGGCCATCATCAAGGAGTTCATGCGCTTC
AAGGTGCACATGGAGGGCTCCGTGAACGGCCACGAGTTCGAGATCGAGGGCGAGGGC
GAGGGCCGCCCCTACGAGGGCACCCAGACCGCCAAGCTGAAGGTGACCAAGGGTGGC
CCCCTGCCCTTCGCCTGGGACATCCTGTCCCCTCAGTTCATGTACGGCTCCAAGGCC
TACGTGAAGCACCCCGCCGACATCCCCGACTACTTGAAGCTGTCCTTCCCCGAGGGC
TTCAAGTGGGAGCGCGTGATGAACTTCGAGGACGGCGGCGTGGTGACCGTGACCCAG
GACTCCTCCCTGCAGGACGGCGAGTTCATCTACAAGGTGAAGCTGCGCGGCACCAAC
TTCCCCTCCGACGGCCCCGTAATGCAGAAGAAGACCATGGGCTGGGAGGCCTCCTCC
GAGCGGATGTACCCCGAGGACGGCGCCCTGAAGGGCGAGATCAAGCAGAGGCTGAAG
CTGAAGGACGGCGGCCACTACGACGCTGAGGTCAAGACCACCTACAAGGCCAAGAAG
CCCGTGCAGCTGCCCGGCGCCTACAACGTCAACATCAAGTTGGACATCACCTCCCAC
AACGAGGACTACACCATCGTGGAACAGTACGAACGCGCCGAGGGCCGCCACTCCACC
GGCGGCATGGACGAGCTGTACAAGTAA
```

C. GPR1 cDNA Accession number: NM_001180094.1

```
ATGATAACTGAGGGATTTCCCCCGAATTTAAACGCGTTGAAAGGGTCATCCTTACTA
GAAAAGAGAGTTGATTCTCTCCGACAGCTTAACACTACCACGGTTAACCAGCTGCTG
```

GGGTTGCCGGGGATGACCTCTACATTCACGGCTCCGCAACTGTTGCAGTTAAGAATA
ATAGCTATAACTGCGTCTGCCGTGTCCCTTATTGCCGGTTGCCTCGGAATGTTCTTC
CTTTCTAAAATGGATAAGAGACGAAAAGTCTTCAGACATGATCTCATCGCATTTTTG
ATAATTTGCGACTTTCTTAAAGCTTTTATTCTGATGATTTATCCCATGATTATCCTT
ATTAATAATAGTGTGTATGCAACACCTGCATTTTTTAATACCTTGGGTTGGTTTACG
GCCTTTGCCATCGAAGGTGCAGACATGGCCATAATGATATTCGCCATACATTTTGCT
ATTTTGATCTTCAAGCCTAATTGGAAATGGCGAAATAAAAGATCGGGAAATATGGAG
GGTGGCTTGTACAAAAAAAGGTCATATATCTGGCCAATTACTGCATTAGTACCTGCC
ATTTTAGCAAGCTTAGCCTTCATTAATTATAATAAACTCAATGACGATTCTGACACC
ACTATTATACTGGATAATAATAACTACAACTTTCCCGATTCTCCCAGGCAAGGTGGC
TACAAACCTTGGAGTGCATGGTGCTATTTACCACCCAAGCCGTACTGGTATAAAATT
GTTTTAAGCTGGGGTCCCAGATATTTCATTATTATTTTCATATTTGCAGTCTACCTC
AGTATTTATATTTTCATTACCAGTGAAAGTAAAAGAATTAAAGCGCAAATTGGAGAC
TTTAACCATAACGTACTAGAGGAAGAGAAAGAAAAGAAAAAATTATTTGGGCTCGGT
CACTGGGGAAAAGCCAAATGGTATTTCAGATCCTATTTTAAATTGCCATTGCTACAT
CTTTTGAGAAATTTAAAGAATTTTTTCACCATTTCGTTCATAGATCCGAATGAGGAA
ACAGACGATTCAGGTAGTAGTAATGGAACTTTCAATTTTGGTGAGAGTTCGAATGAG
ATACCTACACTATTCAGAAAAACAAATACAGGTAGTGATGAGAATGTCTCGGCAAGT
GGTGGAGTTCGCTTACTTGACTATAACAGTGCTAAACCACTCGATATGTCCAAATAT
GCAATGTCTGAACAGCCAGATTTGGAAAGAAATAATCCTTTTGATTGTGAAAATGAC
ATCACACTCAATCCTTCGGAACTAGTATCCAAGCAAAAGGAGCATAAAGTTACTTTT
AGTGTTGAAAATGAAGGACTGGATACAAGAAAAAGTTCAATGCTGGGACATCAGACT
TTCTCTTGCCAAAATTCTCTAGAATCTCCTTTAGCAATGTATGATAATAAGAACGAT
AACAGCGACATAACTAGTAACATTAAGGAAAAAGGAGGCATCATCAACAACAACAGT
AACAACGACGACGACGACAACAACAACAATAACGATAACGATAACGATAACAATAAT
AGCAATAATAATAATAACAATAATAATAATAACAATAATAATAATAACAATAATAAT
AACAATAACAACAACAACAACAATAATAATAATAATAGTAATAATATTAAAAATAAC
GTTGATAACAATAATACTAATCCAGCCGATAATATTCCTACACTTTCTAATGAAGCA
TTTACTCCGTCTCAACAATTTTCACAGGAGAGAGTGAATAATAATGCAGACAGATGC
GAAAATTCAAGTTTCACCAACGTACAACAGCATTTCCAAGCCCAAACCTACAAACAA
ATGAAAAAACGTAGGGCACAAATTCAAAAGAATCTAAGGGCAATATTCATTTATCCA
CTGTCGTATATTGGGATATGGCTTTTCCCCATCATTGCAGATGCGTTGCAATACAAT
CATGAAATAAAGCATGGGCCTACCATGTGGGTGACATACATTGACACTTGCGTTCGA
CCATTAAGTTGTCTCGTCGACGTCATTGTTTACCTGTTCAAGGAAAAACCTTGGAAC
TATTCATGGGCAAAAACAGAATCAAAATATCTCATTGAAAAATATATTCTGAAAGGA
GAGCTTGGTGAAAAGGAAATTCTGAAGTTTTGTCACAGCAATTGGGGGAAAAGAGGT
TGGTATTATCGTGGTAAGTGGAAGAAAAGAAAATGCTGGAAATATTCTACAAACCCT
CTGAAGCGTATACTGTGGTTTGTTGAACGCTTCTTTAAACAATTGTTTGAACTAAAA
CTACACTTTAGTTTTTATGACAATTGTGACGATTTTGAATACTGGGAAAACTACTAT
TCAGCCAAAGATTCAAACGATAATAAACGCACAGAATCTGATGAGACTAAAACGAAT
AGTAGCGATCGCTCCCTTCCATCAAATTCACTTGAACTACAGGCAATGCTTAATAAC
ATCACGGCCGAAGAGGTTGAAGTGCCCTTGTTTTGGAGGATCATTCATCATATTCCA
ATGCTTGGCGGAATAGATCTTGATGAGTTAAACAGATTGTTGAAAATACGGTACAAT
AACGACCATTTTTCTCTACCCGGGTTGAAATTTGCATTAAACCAAAATAAAAGTCAC
GATAAACATCAGGACGTCTCAACTAACAGTATGGTCAAATCCAGCTTCTTTTCAAGC
AATATTGTCACAAACGATGATGAGAATAGCATTGAAGAGGATAAGAATTTACGCTAT
TCAGATGCTAGTGCATCTGAAAATTATCTGGTCAAGCCCACAATACCAGGTACGACT
CCTGATCCAATAATTGAGGCGCAGAACGATAATGATAGTAGTGATAGTAGCGGCATA
GATTTGATAGCCTTCTTAAGAAATGGACCATTATAA

APPENDIX B

PRIMERS

A. Primers for *BamHI* and *EcoRI* cut site addition to both ends of GPR1

5'-GAGAGAGAGGAATTCTTATAATGGTCCATTTCTTAAGAAGG-3’
5'-GAGAGAGAGGGATCCATGATAACTGAGGGATTTCCC-3’

B. Primers for GPR1 sequence addition at both ends of cDNAs of full length and split FPs

5’-GAGTTAAACAGATTGTTGAAAATACGGTACATGGTGAGCAAGGGCGAG-3’
5'-CCCGGGTAGAGAAAAATGGTCGTTATTCTTGTACAGCTCGTCCATGCC-3’

C. Sequencing primers

Gpr1_35F	ATTTCCCCCGAATTTAAACG
Gpr1_401F	TACCTTGGGTTGGTTTACGG
Gpr1_888F	CCATAACGTACTAGAGGAAGAGAAAGA
Gpr1_1378F	GGGACATCAGACTTTCTCTTGC
Gpr1_1885F	GGGCAATATTCATTTATCCACTG
Gpr1_2388F	CGCACAGAATCTGATGAGACTAA
Gpr1_2571F	TGTTGAAAATACGGTACAATAACGA
Gpr1_208R	GAAGAACATTCCGAGGCAAC
Gpr1_2687R	TGCTATTCTCATCATCGTTTGTG

EGFP_22F	ATGGTGAGCAAGGGCGAGGAG
EGFP_689R	CGGCATGGACGAGCTGTACAAG
NEGFP_391R	CAGGATGTTGCCGTCCTC
CEGFP_508F	ACTTCAAGATCCGCCACAAC

NmCherry_420R	CCCATGGTCTTCTTCTGCAT
CmCherry_517F	CAAGCAGAGGCTGAAGCTG

APPENDIX C

FRET EFFICIENCY DATA

Table 1 The data collection of wild-type (W303-1A) cells.

Pixel counts	Cell number on image	Mean of FRET efficiency
100322	13	23,242
72113	8	16,323
32951	5	14,732
29045	7	15,616
10726	2	9,765
52900	5	14,923
74443	9	20,848
38231	6	18
59147	12	16,908
41045	13	18,034
9981	3	12,845
3183	1	15,465
4128	2	6,52
7713	3	5,486
3234	1	4,569
3836	2	6,253
10171	3	9,103
5314	3	6,32
7088	4	10,234
3691	1	14,955
20302	7	12,638
16542	4	9,057
17433	5	12,848
55194	9	11,577
43282	11	10,489
14497	1	15,687
1483	1	13,245
13331	3	15,112

11869	1	11,546
9919	1	15,743
6745	1	4,028
25104	4	17,53
49229	8	17,882
61681	8	15,542
83991	9	17,992
32813	5	13,741
37121	6	12,719
52228	9	16,942

Table 2 The data collection of *gpr1Δ* (LK5) cells.

Pixel count	**Cell number on image**	**Mean of FRET efficiency**
9349	9	16,653
17749	7	15,812
20373	8	18,69
15994	12	15,98
29051	11	17,607
11795	6	15,161
26843	11	14,227
50051	13	17,147
20498	11	16,928
50016	13	15,57
29508	13	18,23
11512	3	16,523
11103	2	17,65
10836	4	14,931
20901	2	14,56
15266	4	14,006
8460	3	17,102
1512	1	15,74
2546	1	15,23
4524	2	16,51
2351	1	15,707
5790	2	14,65
2077	1	19,034

6540	2	15,001
3486	2	11,675
19510	7	11,816
31605	10	11,116
45185	4	12,244
28870	7	10,944
37046	9	11,173
28269	4	8,14
27971	7	10,655

Table 3 The data collection of DK102 cells.

Pixel count	**Cell number on image**	**Mean of FRET efficiency**
13984	2	15,862
26075	6	10,988
77873	5	11,532
38188	7	13,692
61962	6	10,016
44051	5	11,473
52127	9	9,71
22741	5	16,39
66883	4	10,792
27368	3	8,43
48774	4	10,372
43904	3	9,429
7530	2	6,293
8528	2	5,374
17737	4	18,89
2350	1	6,762
4315	2	7,013
2527	1	5,109
2046	2	6,375
6064	2	8,077
6507	2	7,413
8857	2	8,908
3017	1	7,004
3190	1	8,519

6823	3	10,929
5296	1	10,305
6914	3	11,146
6039	1	9,472
19442	3	13,155
28663	3	13,568
18846	2	11,234
8353	2	17,009
4724	1	13,151
15841	3	18,427
3261	2	13,835
3536	2	12,191
9834	9	11,739
14831	5	15,698
6535	2	16,361
8314	2	9,997
5940	3	16,663
16218	7	17,965
3186	2	15,424
3363	4	10,209
5124	3	16,414
2604	1	14,608

APPENDIX D

COMPOSITION AND PREPARATION OF YEAST CULTURE MEDIUM

Table F.1 Composition of minus tryptophane and uracil dropout mix stock

Component	Final concentration (g/L)
Adenine Sulfate	0.058
Arginine HCl	0.026
Asparagine	0.058
Aspartic Acid	0.14
Glutamic Acid	0.14
Histidine HCl	0.028
Isoleucine	0.028
Leucine	0.083
Lysine	0.042
Methonine	0.028
Phenylalanine	0.69
Serine	0.52
Threonine	0.28
Tyrosine	0.042
Valine	0.21

MLT, MLU and MLTU Medium Compositions:

MLT (Medium lack of Tryptophan)

20 g/L glucose

10 g/L casamino acids

6.7 g/L YNB w/o amino acids

1.8 g/L Minus (Trp-Ura) Dropout Mix

0.028 g/L Uracil

MLU (Medium lack of Uracil)

20 g/L glucose

10 g/L casamino acids

6.7 g/L YNB w/o amino acids

1.8 g/L minus (Trp-Ura) dropout msix

0.028 g/L tryptophane

MLTU (Medium lack of Tryptophan and Uracil)

20 g/L glucose

10 g/L casamino acids

6.7 g/L YNB w/o amino acids

1.8 g/L Minus (Trp-Ura) Dropout Mix

20 g/L Agar is added for solid media preparation right before autoclave sterilization.

YPD (Yeast Extract Peptone Dextrose) Media Composition

20 g/L glucose

20 g/L peptone

10 g/L yeast extract

20 g/L Agar is added for solid media preparation right before autoclave sterilization.

COMPOSITION AND PREPARATION OF BACTERIAL CULTURE MEDIUM

LB (Lysogeny Broth)

Ingredient	Concentration (g/L)
Tryptone	10
Yeast extract	5
NaCl	5

The pH of the medium is carefully adjusted to 7.0 prior to sterilization.

20 g/L Agar is added for solid media preparation right before autoclave sterilization.

APPENDIX E

BUFFERS AND SOLUTIONS

10X TBE (Tris-Borate-EDTA) Buffer

108 g/L Tris Base

55 g/L Boric Acid

40 mL/L 0.5M EDTA (pH 8.0)

For agarose gel electrophoresis, 1:10 dilution of stock solution was used.

6X Loading Dye:

10 mM Tris-HCl (pH: 7.6)

0.03% Bromophenol Blue

0.03% Xylene Cyanol FF

60% Glycerol (V/V)

60 mM EDTA

Transformation Buffer I:

100 mL/L 0.3 M KOAc

100 mL/L 1 M RbCl2

10 mL/L 1M CaCl2

50mL/L 1 M MnCl2

15% Glycerol (V/V)

The pH of the buffer is adjusted to 6.5 and filter sterilized.

Transformation Buffer II:

50 mL/L 1 M MOPS

37.5 mL/L 1 M CaCl2

50 mL/L 1 M RbCl2

15% Glycerol (V/V)

The pH of the buffer is adjusted to 6.5 and filter sterilized.

Single Stranded Carrier DNA:

200 mg of salmon sperm DNA (DNA sodium salt from salmon testes, Sigma D1626) was dissolved in 100 mL of TE buffer (Sigma #93283) mixing by a magnetic stirrer for 2-3 hours. 500 µL aliquots were stored at -20°C.

1 M LiAc Solution:

Lithium acetate was dissolved in distilled water and the final pH was adjusted to be between 8.4 and 8.9. Then, it was filter sterilized and stored at room temperature. 100 mM LiAc solution was diluted from the 1 M stock dilution by dilution factor of 10.

50% (w/V) Polyethylene Glycol 3350:

PEG 3350 (Sigma, #P3640) was dissolved in distilled water and the prepared solution was heat sterilized at 120°C for 20 minutes. In order to prevent water evaporation, cap of the stock was sealed with parafilm and the solution was stored at room temperature.